Advanced Review

Polymeric nanoparticles in development for treatment of pulmonary infectious diseases

Young H. Lim,[1] Kristin M. Tiemann,[2] David A. Hunstad,[2,3] Mahmoud Elsabahy[1,4,5]* and Karen L. Wooley[1]*

Serious lung infections, such as pneumonia, tuberculosis, and chronic obstructive cystic fibrosis-related bacterial diseases, are increasingly difficult to treat and can be life-threatening. Over the last decades, an array of therapeutics and/or diagnostics have been exploited for management of pulmonary infections, but the advent of drug-resistant bacteria and the adverse conditions experienced upon reaching the lung environment urge the development of more effective delivery vehicles. Nanotechnology is revolutionizing the approach to circumventing these barriers, enabling better management of pulmonary infectious diseases. In particular, polymeric nanoparticle-based therapeutics have emerged as promising candidates, allowing for programmed design of multi-functional nanodevices and, subsequently, improved pharmacokinetics and therapeutic efficiency, as compared to conventional routes of delivery. Direct delivery to the lungs of such nanoparticles, loaded with appropriate antimicrobials and equipped with 'smart' features to overcome various mucosal and cellular barriers, is a promising approach to localize and concentrate therapeutics at the site of infection while minimizing systemic exposure to the therapeutic agents. The present review focuses on recent progress (2005–2015) important for the rational design of nanostructures, particularly polymeric nanoparticles, for the treatment of pulmonary infections with highlights on the influences of size, shape, composition, and surface characteristics of antimicrobial-bearing polymeric nanoparticles on their biodistribution, therapeutic efficacy, and toxicity.

How to cite this article:
WIREs Nanomed Nanobiotechnol 2016, 8:842–871. doi: 10.1002/wnan.1401

*Correspondence to: mahmoud.elsabahy@chem.tamu.edu and wooley@chem.tamu.edu

[1]Department of Chemistry, Department of Chemical Engineering, Department of Materials Science & Engineering, Laboratory for Synthetic-Biologic Interactions, Texas A&M University, College Station, TX, USA

[2]Department of Pediatrics, Washington University of School of Medicine, St. Louis, MO, USA

[3]Department of Molecular Microbiology, Washington University of School of Medicine, St. Louis, MO, USA

[4]Department of Pharmaceutics, Faculty of Pharmacy, Assiut International Center of Nanomedicine, Al-Rajhy Liver Hospital, Assiut University, Assiut, Egypt

[5]Misr University for Science and Technology, 6th of October City, Egypt

Conflict of interest: The authors have declared no conflicts of interest for this article.

INTRODUCTION

Serious lung infections, such as pneumonia, tuberculosis (TB), and chronic obstructive cystic fibrosis (CF)-related bacterial diseases, are increasingly difficult to treat and can be life-threatening. A number of therapeutics and/or diagnostics have been employed in the management of pulmonary infections. However, poor solubility of some antimicrobial agents, unfavorable pharmacokinetics, lack of selectivity for penetration into diseased tissues, advent of bacteria with multiple drug resistances,[1,2] and, as a result, administration of higher-intensity antibiotic regimens pose significant obstacles to optimizing therapeutics.[3] A promising approach to alleviate these critical barriers in traditional treatment is

the development of engineered nanoparticles (NPs) (i.e., particles in the size range 5–1000 nm) as alternative delivery carriers for a wide range of therapeutics, including drugs, antibodies, proteins, nucleic acids, and various diagnostic agents.[1,4] A wide range of types of NPs, such as dendrimers, lipids, ceramic, fullerenes, and metallic NPs, have been loaded with therapeutic agents and/or imaging probes to improve pharmacokinetics and biodistribution profiles of their small-molecule cargo, aiming to achieve maximum delivery to diseased tissues while reducing exposure of healthy tissues to the introduced materials.[5,6] Among the diverse selection of nanocarriers, NPs constructed from polymeric backbone-structured building blocks offer precise control over their architectures, surface characteristics, and supramolecular assembly.[7] Direct delivery of polymeric NPs, loaded with appropriate antimicrobials and equipped with 'smart' features to overcome various mucosal and cellular barriers, is a promising approach to localize treatment to the site of infection with minimal systemic adverse effects or toxicity from the applied therapeutic agents. This review focuses on recent progress (2005–2015) in the rational development of polymeric NPs for the treatment of pulmonary infections, detailing their chemistry, antimicrobial activity, biodistribution, and toxicity.

LUNGS AS A TARGET SITE

Drugs used for treatment of pulmonary diseases are typically administered via oral, intravenous (IV), or inhalational routes. Among many organs in the human body, the lungs represent an attractive target for local drug delivery due to unique anatomical and physiological features and minimal interactions between the targeted sites and other organs.[8]

Oral (enteral) administration of therapeutics for systemic distribution has been routinely applied for treatment of a broad range of diseases, including pulmonary infections, due to the large surface area (ca. 200 m^2) of the intestinal epithelium and ease of administration, facilitating patient compliance with scheduled dosing.[9] However, the enteral route involves several significant potential complications, such as inhibited absorption of hydrophilic drugs by the epithelial barrier, limited accessibility of the therapeutics to the site of action (i.e., poor distribution), degradation of active moieties during gastrointestinal transit (especially resulting from degradative and proteolytic enzymes and diverse pHs found along the gastrointestinal tract), and toxicity due to nonselective distribution of encapsulated cargo.[10,11] Many of these barriers can be circumvented by parenteral (usually IV) administration. Delivery of pulmonary therapies via the IV route bypasses the need to traverse or diffuse through mucosal barriers, which is a challenge in inhalational treatment approaches.[12] However, the IV approach is an invasive administration route that confers substantial inconvenience, costs, and adverse effects (e.g., central venous catheter complications) over a long course of therapy. Furthermore, both the enteral and IV routes suffer from nonselective distribution and from filtering or metabolism of active ingredients by multiple organ-level clearance mechanisms (e.g., mononuclear phagocytes of the liver and the spleen, or first-pass chemical modification in the liver) before the intended destination in the body is reached.[8] In IV delivery of nanostructures, it is necessary to use submicron particles to avoid adverse effects, such as pulmonary embolism, that may be associated with larger particle size (>5 μm).[13]

In addition to favoring patient compliance, principal advantages of the direct administration of antimicrobials into the lungs via inhalation, relative to oral or IV administration (Figure 1), relate to unique anatomical and physiological features of the lungs that are favorable for drug absorption: large surface area of the alveolar epithelium, ca. 70–140 m^2 in an adult human; high vascularization and thin vascular-epithelial barrier in alveolar region, ca. 0.1–0.5 μm as compared to ca. 20–30 μm of the columnar intestinal epithelium, that mediates considerable permeation and mass transfer with close contact to the central blood circulation; exposure of the lungs to the entire cardiac output (ca. 5 L/min); avoidance of hepatic first-pass metabolism; and relatively lower local proteolytic activity as compared to that of the gastrointestinal tract.[14–16] In this last regard, inhalation represents an attractive alternative to IV administration for systemic delivery of inhaled therapeutic macromolecules, such as proteins, peptides, and DNAs or RNAs.[8,17] Furthermore, the pulmonary route allows for 10- to 200-fold greater bioavailability of such macromolecules as compared with other noninvasive routes.[17] Consequently, aerosolized antibiotics have been suggested to avoid the high and frequent dosing of oral and IV antibiotics (and associated systemic effects), enabling the delivery of locally high doses of antimicrobials with more rapid attainment of effective concentrations at the site of infection, without excessive absorption of the therapeutics into the systemic circulation.[8]

Despite these substantial advantages of inhalation treatment, such delivery of relatively small therapeutics typically suffers from their rapid clearance by

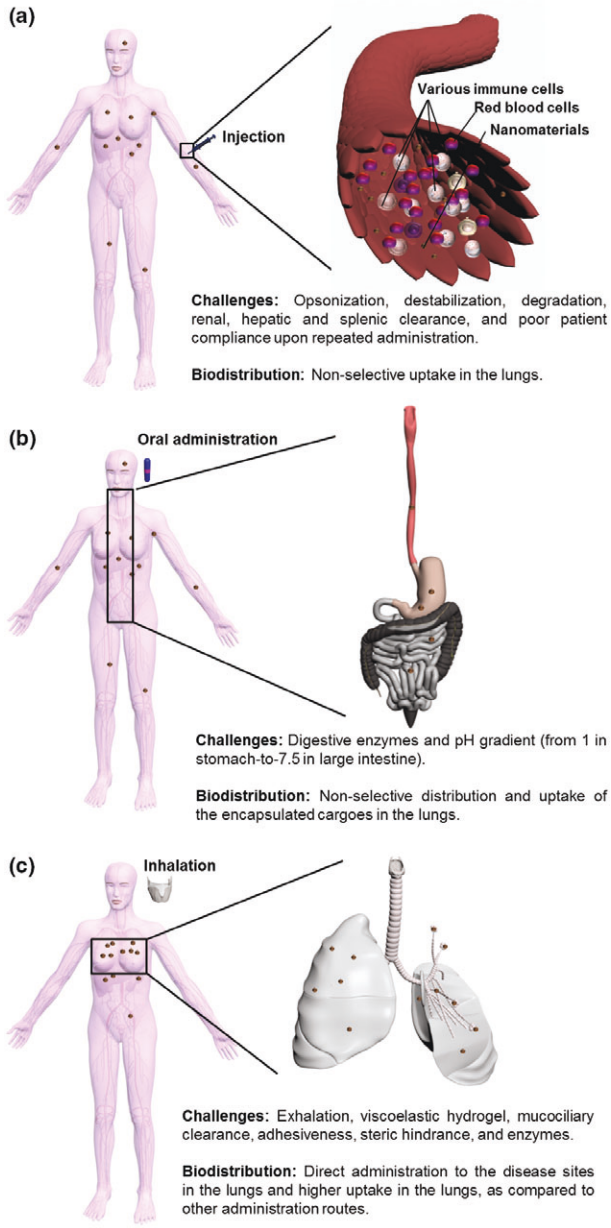

FIGURE 1 | Challenges and biodistribution of nanoparticles following (a) intravenous, (b) oral, and (c) inhalational administrations.

alveolar macrophages upon deposition into the lungs, resulting in a limited amount of residence time and a reduced drug concentration in the vicinity of bacteria.[16,17] Considering the inherent functions of the lungs (i.e., exchange of gas between the blood and the external environment and maintenance of pH homeostasis, not absorption of nutrients), the lung epithelium is not well equipped with transporters and channels as observed in liver and intestine.[15] Additionally, inefficient delivery of the small fractions of inhaled therapeutics deep into the bronchial tree where the mucosal and epithelial barriers have a high resistance, possible degradation of the free drugs, and target non-selectivity of the applied therapeutics are likely to require a higher and more frequent doses of drugs, inducing concerns of systemic toxicity.[18] Additionally, loss of active compounds and/or deformation of particles during generation of inhalable particles may complicate the administration of accurate doses of active ingredients in the final formulation.[19]

PULMONARY DELIVERY OF POLYMERIC NANOCARRIERS: PROMISES VERSUS CHALLENGES

To address the aforementioned limits in the treatment of lung infections, advances in nanomedicine hold great promise for the delivery of therapeutic agents.[20,21] Inorganic NPs, ranging from ceramic to metallic, showed their potential pulmonary applications in the field of magnetic resonance imaging and stimuli-responsive therapeutic and/or diagnostic delivery, but limited surface chemical availability, instability, and poor biocompatibility are drawbacks.[22,23] Various types of particles in nano-sized systems (from organic to inorganic to metallic) present maximized incorporation of targeting ligand and protective coating at their periphery, but the usage of inorganic or metallic NPs for pulmonary application is rather limited to their use as imaging agent. On the other hand, polymeric NPs, in general, offers precise control over particle composition, size, and structure contributing to the improved pharmacokinetics, enhanced aqueous solubility of insoluble hydrophobic drugs, stabilization of therapeutic agents against possible hydrolytic and/or enzymatic degradation, feasibility to incorporate surface decorating moieties (e.g., cell-targeting peptides) onto the particle, mediation of sustained and/or stimuli-responsive release of the payloads, and mimicking natural nanosystems (e.g., viruses, lipoproteins, and proteins) for cell-specific targeted delivery with increased bioavailability.[7,24]

Yet, major challenges associated with pulmonary NP delivery include formulation of particles into a desired size range, durability of NPs against shear forces during nebulization, deposition of particles onto the intended sites, mucociliary clearance, steric hindrance, adhesiveness, and enzymatic activity of the mucus gel or sputum, uptake by alveolar macrophages, and internalization of particles into epithelial

cells.[25,26] For instance, delivery of drugs or nucleic acids loaded within nanocarriers into the airways for treatment of CF-related bacterial infections is typically inefficient, ascribed mostly to the presence of sputum having a bulk viscosity ca. 10^5 times greater than water.[26,27] As a delivery carrier, destabilization of NPs can be a direct consequence of drug leakage, disassembly and/or biodegradation of the particles, detachment of surface-decorating moieties, and opsonization.[28] Even though the drug encapsulation-strategy into NPs has shown superiority in targeting and sustained release, as compared to free drugs, it still suffers from rapid and nonselective NP clearance by the mononuclear phagocyte system (MPS) upon deposition in the lungs.[29] For effective treatment of intracellular infections, such as TB, pneumonia, and aspergillosis, the inhaled therapeutic particles would have to effectively reach the macrophages, which bacteria and fungi utilize as a breeding ground, at therapeutic levels.[30,31] Furthermore, exhalation, effects of degradation products, cytotoxicity, and immunogenicity should be also accounted for in the design and administration of polymeric NPs for treatment of respiratory diseases.[32]

BIODISTRIBUTION: EFFECTS OF SIZE, SHAPE, AND SURFACE CHEMISTRY OF POLYMERIC NPS

Physicochemical characteristics of the particles, such as size,[33–36] shape,[37–39] surface charge,[40,41] and composition[29,42] influence their biodistribution, (sub)cellular internalization, and toxicity.[43–46] Numerous studies have attempted to address the effects of these factors individually; however, what is not fully understood is the interdependent role(s) of these determinants for the intracellular fate of NPs, with some exceptions.[39,47,48] The degree of success in effectively delivering nanotherapeutics to various anatomic sites hinges strongly on the attributes of the applied delivery carriers; for instance, size plays a predominant role in achieving deep-lung deposition of inhaled NPs, while carrier stability in traversing the harsh gastrointestinal environment should be also considered in NPs intended for oral administration. In the meantime, the antimicrobial activity of therapeutic NPs via IV administration depends on the capabilities of NPs to internalize into specific cellular and/or sub-cellular compartments and to remain stable during blood circulation. In the following sections, the effects of size, surface charge, and other important variables on the biodistribution and therapeutic efficacy of polymeric NPs will be highlighted.

Effects of Particle Size and Surface Properties on Distribution Following IV Administration

It is generally accepted that the diameter determines the tissue distribution of spherical particles. Spherical particles smaller than ca. 5 nm become rapidly cleared from blood circulation through extravasation or renal clearance, and those larger than 15 μm are eliminated by mechanical filtration in lung capillary beds, posing risk for pulmonary embolism. Spherical particles in the range of ca. 5 nm to 5 μm in diameter are taken up by the MPS in liver, spleen, lung, and bone marrow following IV administration.[49,50]

Particle surface is often modified into hydrophilic and/or charged characteristics to improve the blood circulation time by avoiding MPS uptake (e.g., PEGylation), to enhance cellular uptake and endosomal escape (e.g., positive charge), or to change hydrophilicities and/or conformations at different pH values (e.g., negative charge).[7] Nevertheless, this surface modification strategy does not appear to be valid for targeted lung delivery following IV administration, as seen with lack of targeted *in vivo* biodistribution of PEGylated or charged NPs via intravenous route of administration.[51–53] Upon IV injection of carboxyl-coated PS spheres in three different sizes, ca. 20, 100, or 1000 nm into F344 female rats, all three types of particles deposited mostly in liver, spleen, and lung, and the proportion of particles of ca. 100 and 1000 nm in the spleen increased significantly over time due to their clearance via the MPS.[54] Among three particles recovered in the uterus and ovary, 20-nm particles showed a longer circulation than 1000-nm particles with two orders of magnitude increases in the number from 1 h to 28 days post-injection. This report was consistent with the data seen with short-term distribution, at 30 min, of amino-modified PS particles injected into mice, where 1000-nm spherical particles showed a faster clearance, ca. 85%, from the blood and higher uptake by the liver, as compared to ca. 60% of 100-nm particles.[55] Small fractions, ca. 1–3%, of both particles in different sizes were found in the spleen.

Formulating particles in micron size could be ideal to achieve passive targeting by venous filtration and entrapment into the capillary beds of the lungs after IV administration.[50] A few recent studies demonstrated preparation of NP aggregates in micron size. For instance, Sinko et al. prepared poly(ethylene glycol) (PEG)-stabilized aggregated nanogel particles (SANPs) with a size of ca. 30 μm, where the crosslinker, 1,6-hexane-bis-vinylsulfone, was programmed to be degraded by enzymes, such

as matrix metalloproteinase-2 present in the lungs, and the subsequent PEG monomers could be eliminated by renal filtration.[56] The particles accumulated selectively in the lungs (primarily in alveolar regions) in rats within 30 min following tail vein injection, and the majority of them remained in the lungs for 48 h. In contrast, controls (i.e., free dyes) were rapidly eliminated (<30 min) from the body upon injection. The enzymatically degraded products were found in the urine after elimination by renal filtration. In another study, Sinko et al. highlighted the size effects of polystyrene (PS) NPs of ca. 2–10 μm in diameter on lung-targeting efficiency, intra-lung distribution, and retention time after IV administration to rats, where microparticles (MPs) with diameter between ca. 6 and 10 μm were claimed to be the optimal size for transient but highly efficient targeting to pulmonary capillaries.[50] Prud'homme et al. prepared lung-targeting composite gel MPs (CGMPs) in the size range of 10–40 μm, composed of ca. 100 nm in a PEG gel matrix.[57] Following tail vein injection of ca. 16 μm CGMPs in mice, uniform and selective delivery of CGMPs to the lungs was observed without off-site deposition in the heart, kidney, spleen, or liver. Meanwhile, hydrolysis of ester bonds in the network allowed for complete degradation of CGMP after 55 days in aqueous solution, which was promising to improve the retention time in the lung for sustained delivery.

Effects of Particle Size and Surface Properties on Distribution following Pulmonary Administration

The distribution of particulates following inhalational administration is highly particle size-dependent.[58] In general, inhaled particulates with aerodynamic diameter (d_{aer}) between 0.5 and 5 μm deposit in the central and distal tracts, while those > 5 μm become trapped in the upper airways (i.e., mouth, trachea, and main bronchi) and those < 0.5 μm are mostly exhaled.[59] As d_{aer} of the particle formulation could be directly influenced by the aerosolization mode, interplay between the design of aerosol particles and the choice of aerosolization mode should be carefully considered. Detailed information on the type, development history, mechanism, and characteristics of aerosol delivery devices, including nebulizer, metered-dose inhaler, and dry powder inhaler, have been discussed in other review articles.[16,60–62]

Upon particulate deposition, transport of polymeric NPs across a thick mucus layer (as found in CF patients) first depends on particle size, typically permeable only for NPs ca. 30–500 nm in diameter.[63,64] Modification of the particle surface may help avoid retention and clearance in the mucus, thereby allowing for enhanced drug delivery.[26] Hanes et al. assessed the different diffusion rates of uncoated carboxyl-modified (muco-adhesive) or PEGylated (e.g., 2 or 5 kDa) (muco-inert) PS NPs on *ex vivo* fresh murine tracheal tissue mucus layers, where 100 nm muco-inert NP diffused successfully while 100 nm muco-adhesive NPs were immobilized.[65]

Meanwhile, mucociliary clearance of particles trapped in the pulmonary mucus blanket appears to be independent of size (ca. 50 nm up to 6 μm), shape (spheres and rods), and surface charge (ca. −50 to +50 mV) of particles. Lehr et al. claimed that the equally efficient mucociliary clearance of particles with varying size and surface characteristics was ascribed to the immobilization of such particles inside the mucus blanket, upon tracking the trajectories of inhaled particles in the mucus blanket *ex vivo* and *in silico*.[66,67] Instead, the chemical property of NP determined the mucociliary clearance rate based on a trachea-based *in vitro* model using NPs. Particles, in the range of ca. 50 nm to 6 μm in size and ca. −42 to +47 mV in zeta potential, composed of different PLGA-based copolymers showed significant effect on particle clearance in contrast to PS particles displaying no difference.[67] Particularly, PEG-PLGA particles exhibited the fastest transport rates (i.e., ca. 5.9 ± 1.7 mm/min) and mucoadhesive chitosan-PLGA particles were transported at the slowest rate (i.e., ca. 0.7 ± 0.3 mm/min) among tested NPs. In another study, Brody et al. observed rapid clearance of polyacrylamide-based hydrogel MPs of 1–5 μm in diameter by mucociliary transport and through the circulation as opposed to prolonged lung retention of 20–40 nm counterparts, enhanced by cell-penetrating peptides, nona-arginine, following intratracheal administration.[68]

Effect of Particle Size, Shape, and Surface Properties on Clearance by the MPS following Pulmonary Administration

It is generally understood that increasing the particle size leads to the higher possibility of phagocytosis by macrophages. Mitragotri et al. demonstrated this particle size-dependent alveolar phagocytosis in rats (e.g., the maximal phagocytosis and attachment with particles in the size range of ca. 2–3 μm).[33] In concert with this finding, Makino et al. observed a higher degree of alveolar macrophage uptake with PS particles with a diameter of 1 μm than those with

diameters <500 nm or >6 μm.[69] Meanwhile, trapping of PS particles of 1 μm in diameter by alveolar macrophages was also influenced by their surface properties; particles displaying primary amines were most effectively trapped as compared to those functionalized with carboxyl, sulfate, or hydroxyl groups. Based on this information, more effective uptake and therapeutic action of NPs might be achieved with NP size < ca. 500 nm in diameter to avoid the alveolar macrophages, unless intended. On the other hand, DeSimone and Ting et al. reported more uptake of smaller particles of ca. 80 × 320 nm *in vivo* by monocytes and macrophages than larger particles of ca. 6 μm diameter, using PLGA or PEG hydrogel particles prepared by Particle Replication in Nonwetting Template (PRINT) fabrication process.[70] More recently, three sizes of PEGylated PRINT nanogel particles (i.e., 80 × 320 nm, 1.5, and 6 μm donuts) showed increased lung residence time, with the largest increase in residence time for the smallest 80 × 320 nm particles, upon instillation in the airways of C57BL/6 mice.[71] These particles were retained in the lung for at least a month without obvious inflammation.

Mitragotri et al. highlighted the complex interplay between size and shape of particulates in phagocytosis by alveolar macrophages, using six different types of PS particles (i.e., spheres, oblate ellipsoids, prolate ellipsoids, elliptical disks, rectangular disks, and UFO-shaped particles).[33,39] Rapid internalization in < 6 min of elliptical disks occurred when their long axis began to attach perpendicularly to cell membrane, causing a symmetrical spread of the membrane around the particle. In the meantime, attachment of the short-axis (flat) side of the particle to cell membranes did not induce observable phagocytic activities. This study concluded that phagocytosis or simple spreading on the particle was determined by the local particle shape at the point of initial contact by macrophages, not by size. Meanwhile, particle size dictated the completion of phagocytosis if the particle volume was larger than the macrophage volume. Other studies by the same group illustrated the maximum initial attachment of elongated particles, in the range of ca. 2–3 μm, to macrophage surface as compared with that of spherical particles, which was not directly related to their phagocytic uptake efficiency.[72,73] Taken together, spheres or oblate ellipsoids may be most suitable for targeting macrophages (e.g., in the case of intracellular infections such as TB) via pulmonary administration, while elongated shapes may help to achieve prolonged blood circulation and avoidance of macrophage uptake, suitable for IV administration.

Effect of Particle Size and Surface Property on Translocation from the Lung to Extrapulmonary Compartments

The combined effects of size, surface charge, and NP composition on the ability to translocate from the lungs into the lymph nodes and bloodstream and on their *in vivo* fate were investigated following lung instillation in rats of inorganic/organic hybrid or organic NPs, engineered with varying chemical compositions, sizes, and surface charges.[74] The limited translocation of NPs with diameter greater than ca. 38 nm from the lung to extrapulmonary compartments of the body at 30 min after administration could be due to mucociliary and/or macrophage-mediated clearance. A small amount of the NPs < ca. 5 nm in diameter migrated rapidly to lymph nodes within 3 min, reached the kidneys and were ultimately excreted into urine by 30 min after administration. Only NPs with a size threshold of ca. 34 nm, regardless of chemical composition and shape, rapidly translocated from the alveolar luminal surface into the septal interstitium, the regional draining lymph nodes, and, finally, the bloodstream.

Notably, the biodistribution of NPs of size < ca. 34 nm was governed by charge effect, where zwitterionic, anionic, and neutral surfaces resulted in a higher transepithelial translocation, in contrast to the limited penetration of cationic NPs. NPs with size < ca. 6 nm and zwitterionic surface translocated from the alveolar airspaces to the bloodstream and were, finally, cleared via renal filtration. Based on these observations, the authors claimed that the use of noncationic NPs with the size range of ca. 6–34 nm would have the highest potential of achieving optimal delivery to the lungs via pulmonary administration route. With respect to this biokinetic analysis on the fate of intratracheally-instilled NPs, Kreyling et al. pointed out that quantitative investigation including a differentiation between transport to the blood through lymphatic drainage and direct translocation across the air-blood barrier to the blood should be pursued.[75] Additionally, employing highly-functionalized NPs with targeting, therapeutic and diagnostic molecules may induce different consequences from the results observed here. Reineke et al. also compared the translocation and organ distribution of relatively larger PS NPs of ca. 50–900 nm in diameter upon pulmonary administration into mice.[76] NP size influenced the rate and extent of NP uptake, in which larger NPs of ca. 250 or 900 nm displayed the highest total uptake (15% of administered dose) at 1 h, whereas smaller NPs of ca. 50 nm had the highest total uptake of ca. 24% at 3 h. The

highest deposition of NPs of all sizes tested was found in the lymph nodes than other tissues, accounting for a total of ca. 35–50% of absorbed NPs.

Nanoparticle-In-Microparticles Formulations for Pulmonary Administration

Micron-sized particles can also be formulated and administered via the pulmonary route to reach the deep lungs. Ungaro et al. developed PLGA NPs of ca. 250 nm in diameter embedded in an inert microcarrier made of lactose, referred to as *nano-embedded microparticles*, ranging from ca. 11–12 μm in diameter, as a pulmonary delivery system for tobramycin.[77] *In vivo* biodistribution studies revealed that NP deposition was dependent on NP composition: chitosan (CS)-modified particles, having more difficult particle dispersion in the air flux than poly(vinyl alcohol) (PVA)-modified counterparts, were found in the upper airways, lining lung epithelial surfaces whereas PVA-modified NPs reached the deep lung. However, surface coating with PVA could be problematic for penetration across mucus. Hanes et al. reported immobilization of PVA-coated PS NPs with speeds at least 4000-fold lower in fresh human cervicovaginal mucus (having similar biochemical and rheological properties as pulmonary mucus) than in water, regardless of PVA molecular weight (MW) or incubation concentration.[78] Similarly, the transport of NPs of PLGA or PEG-*b*-PLGA coated with PVA also slowed at ca. 29,000- and 2500-fold, respectively, compared to their uncoated counterparts.

Despite the promising results of nanoparticle-in-microparticles as pulmonary delivery carriers, particles of micrometer scale are prone to slow diffusion and to uptake by alveolar macrophages, which, consequently, may hamper their effectiveness as drug delivery carriers for inhalation administration.[60]

Effect of Size, Surface Charge, and Composition of Particles on Diffusion Through Pulmonary Mucus

Size-dependent particle diffusion through the ca. 220 μm-thick mucus was investigated *in vitro* by De Smedt et al., where CF sputa almost completely blocked the transport of all tested PS-based spherical NPs of ca. 120–560 nm in diameter, having similar negative charges, ca. −50 mV, over 150 min.[63] The mass percentage of NPs that diffused through CF sputum was ca. 1.3-, 6.8-, and 42-fold smaller for 120-, 270-, and 560-nm NPs, respectively, as compared with their diffusion through buffer. The different transport rates of NPs of varying sizes was probably due to greater steric obstruction in the CF sputum, possessing pores ca. 100–400 nm in diameter, with increasing particle size. There was an interesting observation—a higher degree of NP diffusion through the more viscous sputum samples, which might be due to structural changes in CF sputum network (i.e., having a more macroporous structure when the sputum becomes more viscoelastic).

In addition to size, the diffusion of polymeric NPs in respiratory mucus is highly sensitive to NP surface characteristics. When comparing the mean diffusion coefficients of amine-modified and carboxylated PS particles, in the diameter range of ca. 100–500 nm, on transport in human CF sputum, amine-modified (neutrally-charged) NPs underwent more rapid transport than the carboxylated (negatively-charged) particles because of their reduced electrostatic adhesiveness.[64] Similarly, De Smedt et al. reported the hindered mobility of charged NPs of ca. 100 nm or 200 nm in size, either positively or negatively charged, in bacterial biofilms and CF sputum, while their PEGylated neutral counterparts showed increased mobility.[79] This particle surface chemistry-dependent mucus penetration was, in part, due to the altered rheological properties of the mucin network. Chin et al. found that positively-charged PS NPs could crosslink the mucin network, resulting in the formation of viscous mucus and impediment of mucin gel hydration.[80] In contrast, carboxyl-functionalized counterparts enhanced the dispersion of aggregated mucin, perhaps due to the combined effects of electrostatic repulsion, chelation, reduction in intra/inter-mucin hydrogen bonding density, and network hydration. These results indicate the influence of NP surface charge on mucus penetration and transport during pulmonary administration.

The rapid penetration of polymeric NPs through highly viscoelastic mucus was demonstrated by coating them densely with low MW PEG, preventing the hydrophobic core of NPs from adhering to the hydrophobic domains of the mucin and minimizing the interaction between the neutral, nonmucoadhesive PEG-containing NP surface and the polyanionic mucus contents.[81,82] Hanes et al. reported that PEG-coated NPs of ca. 100 and 200 nm in diameter rapidly penetrated respiratory mucus by ca. 15- and 35-fold than their uncoated counterparts, respectively, while NPs of size larger than ca. 500 nm in diameter were sterically immobilized by the mucus mesh.[83] The densely PEG-coated PS NPs of ca. 200 nm in diameter displayed ca. 90-fold higher geometric mean effective diffusivity (D_{eff})

due to their minimized interaction with CF sputum constituents, as compared to similarly sized, uncoated NPs.[84–86]

Importantly, the penetration of NPs of 200 nm in diameter across the CF sputum was more feasible when they were coated with PEG with MW between 2 and 5 kDa,[86] whereas NPs coated with 10-kDa PEG were mucoadhesive.[87] Transport of both coated and uncoated NPs of ca. 500 nm was hindered; this selective penetration, in agreement with another study,[64] was partially due to the average 3D mesh spacing of CF sputum, i.e., ca. 140 ± 50 nm (range: 60–300 nm[86] or 100–400 nm[63]).[86] In the meantime, the smaller curvature of ca. 100 nm NPs did not appear to provide a sufficient PEG coating to be mucus inert, resulting in their more hindered transport in CF sputum as compared to ca. 200-nm NPs.

De Smedt et al. also demonstrated effective diffusion of PEG-coated NPs of ca. 200 nm in diameter across the *P. aeruginosa* biofilm extracellular polymeric substance matrix, in contrast to the hindered diffusion of their noncoated and charged counterparts.[79] Interestingly, they observed ca. 15- and 400-fold lower D_{eff} of ca. 200 and 500 nm PEG-coated particles, respectively, in CF sputum than in cervicovaginal mucus, demonstrating elevated adhesive and obstructive properties unique to the CF sputum mesh.[25,26]

Hanes et al. applied the PEGylation strategy to partially biodegradable polymeric NPs, composed of poly(sebacic acid) (PSA) and 5-kDa PEG.[84] A rapid penetration of NPs of PSA-*b*-PEG, with an average hydrodynamic diameter of ca. 170 nm (i.e., a ca. 50-fold greater transport rate than uncoated counterparts at a time scale of 1 s) in sputum expectorated from the lungs of CF patients was ascribed to the efficient partitioning of the muco-inert PEG coating to the particle surface.

The surface modification of polyethylenimine (PEI)-based nanocomplexes with PEG has been broadly employed for pulmonary delivery of nucleic acids in CF to alleviate electrostatic association of cationic particulates with negatively-charged mucus constituents. Hanes et al. reported rapid penetration of highly compacted, densely PEG-coated DNA/PEI NPs in the human CF mucus *ex vivo* and mouse airway mucus *ex situ*.[88] In addition to enhanced particle diffusion and distribution of gene carriers in mouse airways, densely PEG-coated DNA/PEI NPs delivered a full-length plasmid encoding the CF transmembrane conductance regulator protein in mouse lungs and airways, without causing acute inflammation or toxicity. In contrast, Kissel et al. observed only moderate gene expression *in vivo* and severe lung inflammation from PEG-grafted PEI/DNA despite its efficient transfection in cell culture.[89]

Optimization of the degree of PEGylation and PEG MW should be carefully executed for efficient mucosal drug delivery. For example, Saltzman et al. observed improved diffusion, up to 10 fold, of ca. 170 nm-PLGA NPs upon PEG surface coating in human cervical mucus, where their diffusion was strongly dependent on both PEG MW and density on the particle surface.[90] Varying MW of PEG was tested to reduce the mucoadhesion of highly compacted DNA NPs, composed of single molecules of plasmid DNA complexed with PEG-*block*-poly(L-lysine) NPs ($CK_{30}PEG$).[91] Even though $CK_{30}PEG_{5k}$ and $CK_{30}PEG_{10k}$ DNA NPs displayed resistance to DNase I digestion and high gene transfer to the lung airways of mice after inhalation, immobilization of all $CK_{30}PEG$ DNA NP formulations in freshly expectorated human CF sputum could be ascribed to insufficient PEG surface density on the DNA NPs, as compared to the mucus-penetrating NPs of PS-*b*-PEG_{2k}. Despite its popular use, recent data have also raised immunogenic concerns with PEGylation, including activation of the immune system and a loss of macrophage-escaping efficacy upon repeated administration.[81,92]

Surface Modification with Mucoadhesive Polymers

As summarized above, the prevailing paradigm in penetrating the human lung mucus secretions has been to employ nonadhesive polymers, such as PEG, at the surfaces of NPs.[84,93] In contrast to this concept, Ungaro et al. employed hydrophilic mucoadhesive polymers, such as cationic CS and nonionic PVA, to modulate interactions between NPs and mucus by increasing their residence time and intimate contact with the mucosa.[77] Increased *in situ* residence of NPs with hydrophilic mucoadhesive polymers was observed, where CS-coated PLGA NPs showed a higher interaction with polyanionic mucus than PVA-engineered NPs due to their stronger electrostatic interaction. The mucoadhesive CS-engineered NPs penetrated the mucus more readily than the PVA-coated NPs in an artificial CF mucus model.

Application of Mucolytic Agents for Efficient Mucus Penetration

Beyond NP coating with nonmucoadhesive or mucoadhesive polymers, enhancement of particle penetration in the CF sputum could also be realized

by lowering the viscosity of pulmonary secretions using mucolytic agents (e.g., recombinant human DNase (rhDNase) or *N*-acetyl cysteine (NAC)) before deployment of NPs containing active ingredients in the lungs.[94,95] To reduce the barrier properties of sputum, proteolytic enzymes such as trypsin have been extensively studied as peptide mucolytics, but nonspecific serine proteolysis could be problematic. Hanes et al. combined the two strategies of applying NAC and modifying NP surface with PEG to synergistically avoid adhesive trapping and aggregation of the NPs in CF sputum.[96] NAC reduces the disulfide bonds linking mucin monomers, resulting in depolymerization of mucin.[25] NAC pretreatment enhanced penetration by the densely PEG-coated 200 nm NPs, with average speeds approaching their theoretical speeds in water. This rapid penetration correlated with increased average spacing between sputum mesh elements (i.e., from ca. 145 ± 50 to 230 ± 50 nm) upon NAC treatment. In contrast, uncoated NPs were trapped in NAC-pretreated CF sputum to the same extent as in native sputum, demonstrating the NAC-facilitated penetration of PEG-coated, muco-inert NPs.

Inhalation administration might allow for pulmonary absorption and deposition of therapeutic macromolecules, such as peptides and proteins, which otherwise must be injected. However, gene carrier diffusion across adhesive and hyperviscoelastic sputum is challenging.[17] Hanes et al. illustrated the enhancement of CF sputum penetration and airway gene transfer of compacted DNA NPs upon pretreatment with NAC.[97] Unlike the highly compacted DNA NPs of poly-L-lysine conjugated with 10-kDa PEG segment ($CK_{30}PEG_{10k}$/DNA NPs) trapped in CF sputum, pre-treatment of lungs with adjuvant regimens consisting of NAC or a combination of NAC and rhDNase increased the average effective diffusivities by ca. 6-fold and 13-fold, respectively, leading to a higher degree of sputum layer penetration of the gene carriers. Gene expression was enhanced up to ca. 12-fold with pretreatment of intranasal dosing of NAC prior to application of $CK_{30}PEG_{10k}$/DNA NPs to the airways of mice with *P. aeruginosa* lipopolysaccharide-induced mucus hypersecretion, as compared to saline control. In another study, the same group highlighted an enhanced diffusion of adeno-associated virus gene vectors (AAV1) in CF sputum upon mucolytic therapy with NAC (i.e., rapid diffusion of > ca. 47% of the applied AAV1 in NAC-treated sputum vs. ca. 5% in untreated sputum).[98] Collectively, these studies demonstrated the potential utility of adjuvant mucolytic therapy with NAC or a combination of NAC and rhDNase prior to administration of a NP gene carrier for promoting improved gene transfer.

Biodistribution of Degradable Particulates Delivered via Pulmonary Route

Biodegradable polymeric NPs have shown to have sufficient drug-loading capacity, sustained drug-release profile, ability to penetrate viscoelastic human mucus, and low immune toxicities.[26,99] For example, a recent pharmacokinetic study by Wooley et al. demonstrated extended lung retention time for near-infrared (IR) dyes conjugated onto amphiphilic block copolymers comprising biodegradable polyphosphoester-based polymeric micelles and their stabilized, shell crosslinked knedel-like (SCK) analogs (e.g., lung extravasation half-life ($t_{1/2}$) of ca. 4.2 and 8.3 days, respectively) as compared to the small-molecule near-IR probe (e.g., $t_{1/2}$ of 0.2 days) upon their intratracheal administration in mice.[100] It was also observed that lung retention of ^{111}Ag was prolonged when ^{111}Ag-radiolabeled species were loaded into similar amphiphilic block copolymer NPs.[101] Although these biodistribution studies provided insights into the understanding of results of increased *in vivo* therapeutic efficacy,[102] there were limitations in the conclusions that could be drawn. Those limitations require further consideration, theoretically and experimentally, in determining the fate of NPs by tracking the probes in terms of their biodistribution and pharmacokinetics because of the possible disassembly of polymeric NPs and subsequent undesired release of probe molecules from NPs, whether covalently conjugated or physically loaded.

Fattal et al. reported that PLGA NPs of different surface charges showed unique patterns of penetration across the mucus layer and internalization by the underlying epithelial cells.[103] While the hydrophilic poloxamer (PF68)-coated NPs resulted in fast diffusion through the mucus layer and high internalization by the cells, the mobility of CS- and PVA-coated NPs was reduced due to interactions with the mucin chains. Decrease in transepithelial electrical resistance was observed only with CS-coated NPs because of their transient and reversible opening of the tight junctions. No increase of *in vitro* MUC5AC gene expression or the protein levels in the Calu-3 cells from all three NP formulations confirmed the nonimpairment of the bronchial epithelial barrier.

Hsia and Nguyen et al. compared *in vitro* cell uptake and *in vivo* pulmonary uptake of naturally- and synthetically-derived biocompatible polymeric NPs for inhalational protein/DNA delivery.[104] While all of six polymeric NPs (i.e., gelatin, CS, alginate,

PLGA, PLGA-CS, and PLGA-*b*-PEG) were cyto-compatible and displayed dose-dependent uptake by type 1 alveolar epithelial cells, PLGA-based NPs had the highest cyto-compatibility and natural polymer NPs showed the highest *in vitro* uptake at specified concentrations. Upon a single inhalation of gelatin or PLGA NPs encapsulating yellow fluorescent protein (YFP) plasmid DNA or rhodamine-conjugated erythropoietin (EPO) into rat lungs, both NPs displayed a widespread EPO distribution for up to 10 days and increasing YFP expression for at least seven days. Overall, the authors favored PLGA and gelatin NPs as promising carriers for pulmonary protein/DNA delivery.

Upon intratracheal instillation of fluorescently-labeled, hydrophobically-modified glycol CS NPs of ca. 350 nm in diameter into mice, the NPs remained in the lungs for the first 24 h with the half-life of fluorescence intensity of ca. 130 h.[105] While there was minor accumulation of NPs in extrapulmonary organs including liver, kidney, spleen, heart, salivary gland, mesenteric lymph node, accessory sex gland, testis, and brain, the fluorescence intensity was at its highest level in the lungs. The concentration of NPs in plasma displayed the maximum level at 1 h after instillation, and returned to control levels by day 7 (half-life in plasma ca. 42 h). The highest level of NP concentration excreted via urine appeared at 6 h after instillation.

In another pathologic examination of tissues after intratracheal instillation of fluorescein isothiocyanate (FITC)-encapsulated PLGA NPs of ca. 240 nm in average diameter, PLGA NPs remained in type 1 alveolar epithelial cells, alveolar spaces, and blood basement membrane for > 1.5 h after administration.[106] Prompt transit through type 1 alveolar epithelial cells and resistance to uptake by macrophages (such as alveolar macrophages and Kupffer cells) were hypothesized, based on immediate detection of encapsulated FITC in the blood. However, tracking PLGA NPs by the detection of FITC has complications in concluding the fate of PLGA NPs due to the likelihood of premature release of free, diffusible FITC from NPs.

Effect of Particle Size and Surface Characteristics of Particles on Cellular Uptake and Internalization

The endocytosis of NPs is strongly dependent on their size and charge. In one study, the clathrin-mediated pathway of endocytosis showed an upper size limit for internalization of particles of ca. 200 nm in diameter, while NPs of greater size relied on caveolae-mediated internalization.[35] In other examples, cationic NPs with larger diameter, in the range of ca. 80–250 nm, took a clathrin-dependent pathway[107] and those < 25 nm in diameter became transported via nonclathrin-mediated routes,[108] while some particles may have used multiple pathways in parallel.[109]

PEGylation could be beneficial not only for enhancing penetration across the mucosal barrier and movement of administered NPs through human CF mucus but also for promoting entry into alveolar epithelial cells. Brody et al. demonstrated that PEGylation of cationic poly(acrylamidoethylamine-*graft*-poly(ethylene glycol))-*block*-polystyrene) (PAEA-g-PEG-b-PS)-based SCK NPs (cSCKs) of ca. 14–25 nm in diameter could alleviate inflammation and enhance entry and uptake of NPs into alveolar type II cells after intratracheal administration.[110] With respect to the enhanced cell entry behavior of cSCKs modified with PEG grafts (1.5-kDa PEG) in lung alveolar epithelial cells and improved surfactant penetration, the authors speculated an altered mechanism of endocytosis of the NPs (i.e., clathrin-independent entry of PEGylated cSCKs as compared to clathrin-dependent entry of non-PEGylated cSCKs), helping to overcome physiological barriers in the alveolar epithelium. This study did not demonstrate an exact mechanism, which would be crucial to understand the effect of PEGylation of NPs on systemic delivery through the pulmonary route. Similarly, endocytosis of cationic non-PEGylated polysaccharide NPs of ca. 60 nm via the clathrin pathway was also observed by Betbeder et al.[107]

Based on the findings of PEG MW-dependent mucus penetration of CK_{30}PEG DNA NPs in the lungs, Hanes et al. compared the intracellular trafficking of CK_{30}PEG DNA NPs, having two different MWs of PEG, 5 or 10 kDa, in BEAS-2B human bronchial epithelial cells.[111] Both $CK_{30}PEG_{5k}$ and $CK_{30}PEG_{10k}$ DNA NPs were able to escape degradative endolysosomal trafficking by entering the cells via a caveolae-mediated pathway, with slower transport, ca. 3- to 8-fold in BEAS-2B cells, compared to clathrin-mediated endocytosis of PS NPs of 100 nm. Rapid accumulation of the two types of NPs in the perinuclear region of cells was shown within 2 h, ca. 38 and 48%, respectively. Meanwhile, there was no significant effect of PEG MW on NP morphology and intracellular transport.

In a study of differential uptake of PS-based particles by human alveolar type 1 cells and primary human alveolar type 2 cells, Kemp et al. found that surface charge, rather than size, could be a key parameter for cell internalization.[112] While particles

of ca. 50 nm and 1 μm in diameter were internalized in equal numbers, internalization of negatively-charged particles occurred at a significantly higher rate, ca. 4.4-fold at 30 min, as compared to positively-charged particles. Similarly, Kissel et al. observed higher *in vitro* cell internalization of anionic NPs of branched polyester, diethylaminopropyl amine-poly(vinyl alcohol)-*graft*-poly(lactide-*co*-glycolide) (DEAPA-PVAL-*g*-PLGA) in the size range of ca. 70–250 nm, despite their low rate of *in vitro* A549 cell association due to electrostatic repulsion between the anionic NPs and the cell membrane.[113] Opposite results were observed with the cationic counterparts, which exhibited high electrostatic affinity for the membrane, albeit without evidence of internalization.

Effect of NP Surface Charge and Hydrophobicity on Toxicity

The surface charge and hydrophobicity of NPs are important determinants of inducing *in vivo* respiratory toxicity (tissue damage, cytokine release, etc.). Benita et al. reported NPs possessing negative surface charge, rather than those with positive surface charge, would be suitable as drug carriers for local delivery following repeated local pulmonary instillation.[114] When they assessed local and systemic effects of PEG-*b*-PLA NPs as a function of surface charge following repetitive instillation in a murine model, anionic NPs of ca. 120 nm in diameter and ca. –30 mV in zeta potential showed reduced local inflammation as compared to cationic NPs of ca. 140 nm in diameter and ca. +30 mV in zeta potential. Increased pulmonary side effects and transient systemic toxicity observed with cationic NPs were attributed to a higher propensity of being captured and bound to sputum components than anionic counterparts. In another study, Fattal et al. compared *in vitro* cytotoxicity and inflammatory response on A549 human lung epithelial cells to three different types of PLGA NPs of ca. 230 nm in diameter, using different stabilizers (*i.e.*, neutrally-charged PVA, positively-charged CS or negatively-charged PF68).[115] While neither significant cytotoxicity nor inflammatory cytokine release was induced by these PLGA NPs on a Calu-3-based model of bronchial epithelium, the higher tendency of internalization and cell metabolic activity of PF68-coated PLGA NPs may underlie their high toxicity among the tested constructs.

Forbes and Dailey et al. related the NP surface hydrophobicity of three different biomaterial types (i.e., PS, poly(vinyl acetate) (PVAc), and PEGylated lipid nanocapsules of either ca. 50 or 150 nm in diameter) to acute respiratory toxicity following pulmonary administration.[116] NPs with higher hydrophobicity (i.e., PS and PVAc) induced acute respiratory toxicity upon single-dose administration, being retained in the surfactant monolayer and inhibiting surfactant function,[117] whereas PEGylated lipid nanocapsules with lower hydrophobicity caused little or no inflammation. Collectively, optimization of surface hydrophobicity should be carefully considered for design of safe pulmonary nanomaterials (Tables 1 and 2).

ANTIMICROBIAL NANOPARTICLES

Silver-based Antimicrobial-bearing System

Cannon and Youngs et al. developed nebulizable L-tyrosine polyphosphate (LTP) NPs of ca. 920 nm in diameter, encapsulating silver-based antimicrobials (i.e., silver *N*-heterocyclic carbene complex (SCC10)) for treatment of the CF-relevant pathogen *P. aeruginosa*.[118] Silver is highly biocidal against a wide range of Gram-positive and Gram-negative bacteria including *Staphylococcus aureus*, *P. aeruginosa*, and *Escherichia coli*.[119,120] The SCC10-loaded LTP particles of ca. 1200 nm in diameter showed potent *in vivo* antimicrobial efficacy, ca. 75% survival rate, against *P. aeruginosa* over the course of several days with only two administered doses over a 72 h period. Fréchet and Cannon et al. then devised smaller, ca. 100 nm in diameter, nebulizable acetalated dextran NPs (Ac-DEX NPs) encapsulating a hydrophobic SCC.[121] Silver-loading capacity of Ac-DEX NPs was increased with an increasing initial feed up to ca. 30%, resulting in encapsulation efficacy up to ca. 65%. Ac-DEX NP formulations demonstrated activity *in vitro* against *P. aeruginosa*, *S. aureus*, and *E. coli*, including the silver-resistant strain *E. coli* J53/pMG101.

In parallel, benefiting from polymeric formulation with precisely controlled architectures, surface characteristics, and supramolecular assembly, Cannon, Youngs, and Wooley et al. designed nebulizable, multifunctional SCK NPs of poly(acrylic acid)-*block*-polystyrene (PAA-*b*-PS) that were loaded with silver cations and/or SCCs.[102] Antimicrobial efficacy of SCK NPs (shell-loaded with silver cations, core-loaded with SCC10, or loaded via both strategies) was evaluated in a mouse pneumonia model of *P. aeruginosa*. Two SCK NP formulations with SCC10 loaded in the core displayed superior antimicrobial activity and efficacy compared to shell-loaded SCK NPs, probably due to the stability of SCC10

TABLE 1 | General Effect of Particle Characteristics (e.g., Size, Shape, and Surface Properties) on the Deposition and Distribution upon IV Administration

Factors	Particle Size (in diameter)	Effects on NP Biodistribution
Particle size (spherical)	<5 nm	• Rapid clearance from blood circulation through extravasation or renal clearance
	5 nm–15 μm	• Uptake by the mononuclear phagocyte system of liver, spleen, lung, and bone marrow • Ideal for efficient targeting to pulmonary capillaries (ca. 6–10 μm)
	>15 μm	• Elimination by mechanical filtration by capillary beds of the lungs • Risk of lung embolism
Particle shape	Discoidal or filamentous (vs. spherical)	• Prolonged circulation • Reduction of clearance by the mononuclear phagocyte system • Possible concerns about obstruction of the pulmonary vessels by elongated particles
Particle surface	PEGylation	• Prolonged blood circulation by avoiding uptake by the mononuclear phagocyte system

allowing for sustained delivery of the encapsulated SCCs. The Ag^+ dosage required to achieve ca. 60% survival rate from SCC10-loaded SCK NPs was 16 times less than that required from the free drug, at 12 h intervals. Interestingly, SCK NPs with shell-loaded silver cation did not show good efficacy *in vivo*, perhaps due to the relative susceptibility of the weakly complexed Ag^+ to precipitation with Cl^- or other counter-ions and/or its reduction to Ag^0. In spite of promising *in vitro* and *in vivo* antimicrobial efficacy data, translational concerns remained regarding long-term *in vivo* accumulation and possible toxicity that may be elicited by the nondegradable NPs.

To address these limits, two new series of potentially fully-degradable polymeric NPs, composed of phosphoester and/or L-lactide, have been designed specifically for silver loading into the hydrophilic shell and/or the hydrophobic core, as potential delivery carriers for three different types of silver-based antimicrobials—silver acetate or two SCCs.[122] Silver-loading capacities of these NPs reached up to ca. 12% (w/w), and kinetic studies of silver-bearing NPs revealed ca. 50% release at 2.5–5.5 h, depending on the type of silver compound loaded. Interestingly, packaging of SCCs in the NP-based delivery system enhanced MICs up to ca. 70%, compared with the SCCs alone, as measured *in vitro* against ten contemporary epidemic strains of *S. aureus* and eight uropathogenic strains of *E. coli*. Meanwhile, degradability of these NPs was demonstrated by assessing the rates of hydrolytic or enzymatic degradation, by structural characterization of the degradation products, and by biological assays.

Cannon and Wooley et al. developed another type of degradable polyphosphoester-based silver-bearing NPs, composed of amphiphilic block terpolymer, poly(2-ethylbutoxy phospholane)-*block*-poly(2-butynyl phospholane)-*graft*-poly(ethylene glycol), for potential treatment of bacterial lung infections.[123] Loading of antimicrobial silver cations was possible via the formation of silver acetylides with different coordination geometries, which allowed for up to ca. 15% (*w/w*) loading and a sustained release over five days. These silver-bearing NPs displayed enhanced *in vitro* antibacterial activities against a series of CF-associated pathogens, *P. aeruginosa*, *S. aureus*, and *Burkholderia* spp., and decreased cytotoxicity to human bronchial epithelial cells *in vitro*, in comparison to free silver acetate.

Other Antimicrobial Polymeric Systems

Nebulization of PLGA NPs, in the size range of ca. 190–290 nm, containing three different anti-

TABLE 2 | General Effect of Particle Characteristics (e.g., Size, Shape, and Surface Properties) on the Deposition and Distribution upon Pulmonary Administration

	Particle Characteristics	Remarks
Deposition pattern in the lungs	5–10 μm	Upper airways (mouth, trachea, and primary bronchi)
	1–5 μm	Secondary bronchi (smaller airways and bronchioles) — Optimal size range for deposition in the central and distal tracts
	1–3 μm	Bronchioles
	0.5–1 μm	Alveoli
	<0.5 μm	Exhaled
Mucus penetration	<Optimal conditions> • Size: < 500 nm • Surface: hydrophilic, neutral, & muco-inert	• Mucus pore size in CF: ca. 100–400 nm • Order in penetration rate: • neutral (e.g., PEG) > negative (e.g., carboxylate) > positive • Mucolytic agents (e.g., NAC) facilitate mucus penetration • Mucociliary clearance of particulates is independent of size and surface charge and can be avoided by increasing their diffusivity in mucus or minimizing mucoadhesion. • Penetration facilitated by PEGylation (2 or 5 kDa) • PEGylation enhances mucus diffusion, prolonged blood circulation, and reduction of clearance by mononuclear phagocyte system.
Alveolar macrophage uptake	<Maximum uptake> • Size: 2–3 μm • Surface: neutral charge	• Order of macrophage uptake rate (surface functionality): primary amine > carboxyl, sulfate, or hydroxyl groups • Higher degree of phagocytosis with increasing particle size • Alveolar macrophage uptake can be avoided with particle size < 500 nm or > 6 μm.
Cellular uptake and internalization	<Optimal conditions> • Size: Nano-size • Surface: neutral or negative	• Charge-dependent endocytosis • PEGylation promotes cell internalization. • Order of surface charge on cell internalization rate: • PEG (neutral) or negative > positive
Translocation from the alveolar luminal surface into the blood stream	<Optimal conditions> • Size: 6–34 nm • Surface: non-cationic	• Order of translocation rate (surface charge): zwitterionic, anionic, or neutral > cationic • Lower opsonization and protein adsorption of non-cationic NPs

tubercular drugs (i.e., rifampicin, isoniazid, or pyrazinamide) showed superior drug bioavailability and reduced dosing frequency for management of *Mycobacterium tuberculosis*-infected guinea pigs, compared with oral and IV administration of the parent drugs.[124] Upon a single nebulization of drug-loaded PLGA NPs, a therapeutic drug level was sustained in plasma for 6–8 days and in the lungs for up to 11 days. The increased relative bioavailability, by ca. 13-, 33-, and 15-fold for rifampicin, isoniazid, and pyrazinamide, respectively, was ascribed to prolonged elimination half-time and residence time upon nebulization of the drug-encapsulated NPs, as compared to oral administration of the parent drugs. In another study by the same group, treatment with only five doses of drug-loaded PLGA NPs at 10-day intervals to *M. tuberculosis*-infected guinea pigs was sufficient for clearance of tubercle bacilli in the lung, whereas 46 daily doses of orally administered drugs were required to achieve equivalent therapeutic efficacy.[125] Rifampicin was formulated into aggregated PLGA NPs of ca. 190 nm in size, namely porous NP-aggregate particles (PNAPs), suitable for aerosol delivery [126] The systemic level of rifampicin delivered to guinea pigs following intratracheal insufflation of PNAPs was detectable for six to eight hours whereas the free drug, delivered without NPs, was not detected even in the lungs at eight hours. The authors speculated that the prolonged residence of PNAP-delivered rifampicin in the lungs was due to the association of drugs with alveolar macrophages or with remaining intact particles in the lungs. However, it will be important to study the fate of PNAPs after pulmonary administration, including macrophage uptake and mucus penetration of particles. When compared with oral administration at equivalent

doses, pulmonary administration of PNAPs to guinea pigs resulted in higher and longer rifampicin plasma concentrations, demonstrating the advantage of pulmonary delivery over oral administration.

A combination of enhanced interaction of anti-TB drugs with *M. tuberculosis*-infected phagocytes and controlled drug release into the infected tissues would be desirable to treat TB effectively.[127,128] Báfica et al. claimed that a direct interaction of PLGA NPs (ca. 180 nm in diameter) carrying an anti-mycobacterial drug, *E*-N^2-3,7-dimethyl-2-*E*,6-octadienylidenyl isonicotinic acid hydrazide (JVA), with *M. tuberculosis* led to high activity against extracellular and intracellular mycobacteria.[129] With significant loading efficiency of JVA in PLGA NPs, up to ca. 80%, association of JVA-loaded NPs with mycobacterial cell walls contributed to enhanced *M. tuberculosis* killing inside macrophages, although the mechanism by which JVA-NPs gained access to *M. tuberculosis* was not clear.

Lipid-Polymer Hybrid NP System

Lipid-polymer hybrid NPs exhibit complementary characteristics of both structural integrity of polymeric NPs and highly biocompatible nature of lipids in liposomes. To improve the biocompatibility and cellular affinity of polymeric NP cores, PLGA is often incorporated into lipid shells.[130] Chono et al. investigated the influence of particle size of liposomes on drug delivery to alveolar macrophages in rats following pulmonary administration. They observed enhanced antibiotic delivery efficiency of PLGA-containing liposomes with increase in the particle size over the range of ca. 100–1000 nm.[131] Hadinoto et al. compared the effect of phosphatidylcholine-coated, lipid-polymer hybrid NPs of ca. 300 or 420 nm in size, encapsulating a fluoroquinolone antibiotic, levofloxacin, against *P. aeruginosa* biofilm cells *in vitro*, with PLGA NPs of ca. 240 nm in size.[132] The presence of the lipid coat contributed to the gradual release of the highly water-soluble levofloxacin over 24 h. Although their affinity toward *P. aeruginosa* biofilms was not improved, the hybrid NPs exhibited a ca. 50-fold increase in anti-pseudomonal biofilm affinity over their nonlipid-coated counterparts. Differences in antibiotic activity, release rate, and biofilm cell detachment between uncoated and lipid-coated polymeric NPs were ruled out as contributing factors to the higher anti-biofilm efficacy of the hybrid NPs; the mechanisms for anti-biofilm enhancement in the lipid-polymer hybrid NPs are yet to be identified.

SMART POLYMERIC NPs

In addition to the advantage of nanosized formulation, polymeric NPs take advantage from their capability to incorporate multi-functional 'smart' ingredients, such as responsiveness to a stimulus, allowing for controlled drug release at specific sites or under applied conditions.[28] Such triggers might include internal stimuli (e.g., reducing environment in the cytosol or endosome) or external stimuli (e.g., temperature, ultrasound, magnetic field, or light).

pH-Responsive Polymeric NPs

Gene therapy via the respiratory tract has gained much attention for the treatment of lung diseases.[25] Hanes et al. formulated pH-responsive rod-shaped PEG-$CH_{12}K_{18}$ DNA NPs of poly(ethylene glycol)-*block*-poly(L-histidine)-*block*-poly(L-lysine) (PEG-$CH_{12}K_{18}$) to transfect cells via clathrin-mediated endocytosis while overcoming inefficient endosomal escape of DNA NPs of PEG-CK_{30}., as observed in other studies.[82,133,134] Incorporation of functional groups, L-histidine, having buffering capacity between pH 5.1–7.4, was designed to facilitate endolysosomal escape via the proton sponge effect.[135] While the terminal PEG chains retained a neutral surface charge, poly(L-histidine) buffered the pH without interfering with DNA compaction by poly(L-lysine). The endowed buffering capacity by insertion of poly (L-histidine) enhanced their gene transfer efficiency without affecting their physicochemical properties. The authors claimed that this gene transfer was mediated via clathrin-dependent endocytosis followed by endolysosomal processing, as compared to the nucleolin-dependent entry of PEG-CK_{30} DNA NPs. PEG-$CH_{12}K_{18}$ DNA NPs displayed enhanced *in vitro* gene transfer by ca. 20-fold over plasmid DNA NPs of PEG-CK_{30}, and *in vivo* gene transfer to lung airways in BALB/c mice by ca. 3-fold at 14 days post administration.

Farokhzad et al. developed vancomycin-encapsulated, pH-responsive, and surface charge-switching NPs of ca. 200 nm in size of triblock copolymer, poly(D,L-lactic-*co*-glycolic acid)-*block*-poly(L-histidine)-*block*-poly(ethylene glycol) (PLGA-*b*-PLH-*b*-PEG), potentially for targeting bacterial cell walls at acidic sites of infection.[136] The overall positive charge on the NP surface upon protonation of imidazole groups on the PLH block segment in acidic pH promoted multivalent electrostatic-induced cell binding capability and drug delivery efficiency. In contrast, cell binding affinity and drug delivery efficiency were partially limited at pH 7.4. NP binding to

bacteria at pH 6.0 increased at ca. 3.5-fold for *S. aureus* and ca. 5.8-fold for *E. coli* as compared with those at pH 7.4. At pH 6.0, a loss of antimicrobial efficacy of vancomycin within NPs of PLGA-*b*-PLH-*b*-PEG was minimal (i.e., ca. 1.3-fold increase in MIC against *S. aureus*) as compared to that of free vancomycin and vancomycin-encapsulated NPs of PLGA-*b*-PEG (i.e., ca. 2.0- and 2.3-fold increase, respectively). Further study on selective targeting of these charged NPs toward bacteria surrounded with negatively-charged host cell membranes at sites of infection should be conducted.

Enzyme-Responsive Polymeric NPs

Development of respirable particulates with adequate d_{aer} that can confer deposition in the deep lung, evasion from macrophage uptake, and rapid penetration into mucus is one of the major challenges in inhalation therapy. Several efforts, including hydrogel MPs with desired respirable d_{aer} when dry but enlargement and swelling upon deposition in the moist lung, were made, but those systems were limited to micron-sized carriers.[137,138] Roy et al. developed a multi-tiered two-stage system, nanoparticle-in-microgel, that was designed to fulfill these requirements on d_{aer}.[139] The swelling of the microgels of ca. 1.9 μm in average geometric diameter in PBS buffer for 24 h allowed for a highly porous internal structure and geometric diameter > ca. 6 μm, providing optimal aerodynamic carrier size for deep-lung delivery. Macrophage uptake of the pre-swelled microgels was effectively avoided *in vitro*, only ca. 12% uptake after 24 h, which was attributed to the hydrophilic and swellable nature of microgels. The enzymatic degradability of the microgels was derived from a trypsin-sensitive di-sulfhydryl peptide (CGRGGC) introduced as a crosslinker in four-arm-PEG-acrylate-10 kDa. A triggered burst release of various types of encapsulated compounds was observed within 30 min upon addition of physiological levels of trypsin, whereas they were retained in the absence of enzyme.

Wang et al. developed a strategy of differential delivery of antibiotics to treat bacterial infections, using a bacterial-lipase sensitive polymeric triple-layered nanogel (TLN) as the nanocarrier.[140] The TLN of ca. 430 nm in diameter and ca. –20 mV in zeta-potential was composed of three compartments: crosslinked polyphosphoester core, bacterial lipase-sensitive poly(ε-caprolactone) (PCL) interlayer, and PEG shell. The presence of PCL prevented premature drug leakage or nonspecific drug release in aqueous solution by surrounding the drug reservoir prior to reaching the sites of bacterial infection. Upon contact with bacterial lipases abundant in microbial flora, degradation of the PCL interlayer induced the release of encapsulated antibiotics. Encapsulated vancomycin was almost completely released from the TLN within 24 h only in the presence of lipase-secreting *S. aureus*, thereby achieving targeted inhibition of *S. aureus* growth. This approach could be applied to on-demand delivery of antibiotics for the treatment of a variety of infections caused by lipase-secreting bacteria (Table 3).

USE OF RED BLOOD CELLS AS NP DELIVERY CARRIERS TARGETING THE LUNG

As delivery vehicles in the circulatory system, unique characteristics of red blood cells (RBCs), including permeability to biological barriers and expression of ligands (e.g., CD47 and CD300) that bind to inhibitory receptors expressed by macrophages, make RBCs intriguing.[28,142] Mitragotri et al. demonstrated 'cellular hitchhiking' of polymeric NPs onto RBCs to avoid MPS clearance and thereby improving the accumulation of NPs in lungs.[143] Reversible, noncovalent attachment of spherical PS NPs of ca. 200 or 500 nm in diameter to RBCs was possible via electrostatic and hydrophobic interactions. For instance, RBCs carried about 24 NPs of ca. 200 nm in diameter per cell at a particle/RBC feed ratio of 100:1. Upon IV administration, NP desorption occurred rapidly, likely due to shear or direct RBC-endothelium contact during their transit through the tissue microvasculature.[144] As a result, ca. 6% of NPs remained on the surface of RBCs in circulation after 30 min. The significant factors affecting the rate of NP detachment appeared to be the size and geometry of vasculature and the location of NP attachment to RBCs. The RBC-adsorbed NPs exhibited blood persistence ca. threefold higher than free NPs over 24 h, leading to ca. sevenfold higher accumulation in lungs. A distinct accumulation profile of RBC-adsorbed NPs in the lungs was observed (i.e., ca. 15- and 10-fold of improvement of lung/liver and lung/spleen NP ratios, respectively). The authors speculated that accumulation of NPs in the lungs was due to mechanical transfer of NPs from the RBC surface to lung endothelium. In contrast, uptake of NPs attached to RBCs was reduced in mononuclear phagocytic organs such as liver and spleen. Conjugation of anti-ICAM-1 antibody to the RBC-adsorbed NPs increased lung targeting and retention over a period of 24 h, indicating a transfer of NPs from RBCs to

TABLE 3 | Studies of Antimicrobial Efficacy of Polymeric Nanoparticles

Targeted disease	NP Composition	Administration Method	Characteristics	Cargoes	Methods	Remarks	Reference
CF-relevant chronic lung diseases	PEG-*b*-poly(L-histidine)-*b*-poly(L-lysine) (PEG-$CH_{12}K_{18}$)	Inhalation	ca. 330 nm (length) & 13 nm (width)	DNA	*In vitro* *In vivo*	• pH-responsive polymer by insertion of poly(L-histidine) moieties having a buffering capacity • ca. 20- and 3-fold improvement of in vitro and in vivo gene transfer, respectively, of PEG-$CH_{12}K_{18}$ DNA NPs over PEG-CK_{30} DNA NPs	82
CF-relevant chronic lung diseases	Poly(L-lysine)-*b*-PEG ($CK_{30}PEG$)	Inhalation	ca. 220–350 nm (length) & 11–15 nm (width)	DNA	*In vitro* *Ex vivo* *In vivo*	• $CK_{30}PEG_{10k}$ and $CK_{30}PEG_{5k}$ NPs displayed the highest gene transfer to lung airways due to the partial protection against DNase I digestion.	91
Pseudomonas infections	Poly(acrylic acid)-*b*-polystyrene	Inhalation	ca. 30 nm	Silver cations & silver *N*-heterocyclic carbene complex	*In vitro* *In vivo*	• SCK NPs formulations with SCC10-loaded in the core displayed a superior antimicrobial activity and efficacy over shell-loaded SCK NPs	102
Pseudomonas infections	L-Tyrosine polyphosphate	Inhalation	ca. 1200 nm	Silver *N*-heterocyclic carbene complex (SCCs)	*In vitro* *In vivo*	• ca. 75% of survival was achieved against *P. aeruginosa* with only two administered doses over a 72 h period.	118
Pseudomonas infections	Dextran	N/A	ca. 100 nm	Silver *N*-heterocyclic carbene complex	*In vitro*	• Degradable acetalated dextran NPs • High drug encapsulation efficacy up to ca. 65%	121
Pseudomonas infections	Polyphosphoester-*b*-poly(L-lactide)	N/A	ca. 25–34 nm	Silver cations & silver *N*-heterocyclic carbene complex	*In vitro*	• Potentially fully-degradable polymeric NPs • Up to ca. 70% of improvement in MIC as	122

TABLE 3 | Continued

Targeted disease	NP Composition	Administration Method	Characteristics	Cargoes	Methods	Remarks	Reference
						compared to the SCCs alone	
Pseudomonas infections	Poly(2-ethylbutoxy phospholane)-*b*-poly(2-butynyl phospholane)-*g*-poly(ethylene glycol)	N/A	ca. 35 nm	Silver cations	*In vitro*	• Potentially degradable polymeric NPs • Up to ca. 15% (w/w) silver loading and sustained release over five days	123
Tuberculosis	PLGA	Oral, IV, or inhalation	ca. 190–290 nm	Rifampicin, isoniazid or pyrazinamide	*In vivo*	• Sustained drug release in the plasma for six to eight days and in the lungs for up to 11 days • Superiority bioavailability of nebulization method to oral or IV administration	124,125
Tuberculosis	PLGA	Oral, IV, or inhalation	ca. 200 nm	Rifampicin	*In vitro* *In vivo*	• Porous nanoparticle-aggregate particle of ca. 2.7 μm • Detection of systemic levels of rifampicin in the lungs for six to eight hours	126
Bacterial infections	poly(D,L-lactic-*co*-glycolic acid)-*b*-poly(L-histidine)-*b*-poly(ethylene glycol)	N/A	ca. 200 nm	Vancomycin	*In vitro*	• pH-responsive, surface charge-switching NPs from poly(L-histidine) segment • ca. 3.5-fold increase of vancomycin-encapsulated NPs displayed in binding to bacteria at pH 6.0 with ca. 2.3-fold enhanced MICs against *S. aureus*.	136
N/A	Crosslinked four-arm-PEG_{10k}	Inhalation	ca. 1.9 μm in dry & >6 μm when swelled	N/A	*In vitro*	• Avoidance of macrophage uptake, ca. 12% of uptake after	139

TABLE 3 | Continued

Targeted disease	NP Composition	Administration Method	Characteristics	Cargoes	Methods	Remarks	Reference
						2 h, of the pre-swelled microgels *in vitro* • Trypsin-triggered drug release upon degradation	
Bacterial infections	Polyphosphoester-*b*-poly (ε-caprolactone)-*b*-PEG	N/A	ca. 430 nm	Vancomycin	*In vitro*	• Bacterial-lipase sensitive nanogel	140
Tuberculosis	PLGA	Oral or inhalation	ca. 350–400 nm	Rifampicin, isoniazid or pyrazinamide	*In vivo*	• Improved antimicrobial activity by using wheat germ agglutinin-functionalized PLGA NPs	141

endothelium in the vasculature. The RBC-mediated circulation time of NPs could be further controlled by modifying NP surface characteristics or by endowing NPs with binding specificity toward RBCs.

SUPERPARAMAGNETIC IRON OXIDE NANOPARTICLES (SPIONs) FOR PULMONARY DELIVERY

Targeted aerosol delivery of superparamagnetic iron oxide NPs (SPIONs), nanomagnetosols, to specific lung regions other than the airways or the lung periphery in combination with a target-directed magnetic gradient field was demonstrated by Rudolph et al.[145] When an aqueous suspension of nanomagnetosols was nebulized via intratracheal intubation to mouse lungs, ca. 3-fold higher lung deposition of SPIONs was achieved under application of the magnetic field. When the magnet's tip was centered directly above the right lung lobe, ca. 8-fold higher relative SPION deposition in the right lobe was observed as compared to that in the left lobe. The potential use of nanomagnetosols in the targeted aerosol drug delivery system was then demonstrated by formulation of plasmid DNA (pDNA) with the SPIONs. Nebulization of the pDNA-SPIONs inure to the lungs of intact mice in the presence of a magnetic field resulted in a ca. 2-fold higher dose of pDNA in the magnetized right lung than in the unmagnetized left lung. Based on these results, application of nanomagnetosols to polymeric NPs could be utilized for targeted delivery toward a desired lung region *in vivo* by a properly positioned magnetic field.

SUMMARY: CHEMICAL DESIGN AND FUTURE DIRECTIONS

Physical and chemical properties determine the lung deposition, mucus penetration, and subsequent biodistribution of administered therapeutic NPs (Figure 2). For example, d_{aer} of NPs is known to be the major physical parameter that influences their deposition site in the lungs, but upon deposition in the lung, combined effects of size and surface properties, such as hydrophilicity and charge, regulate subsequent transport in the mucus and to the epithelial surface. In the design of polymeric NPs for pulmonary delivery, these strategies should be accounted for to maximize their efficacy. The following sections focus on the particle features in nanometer scale that allow for delivery of therapeutics via pulmonary route.

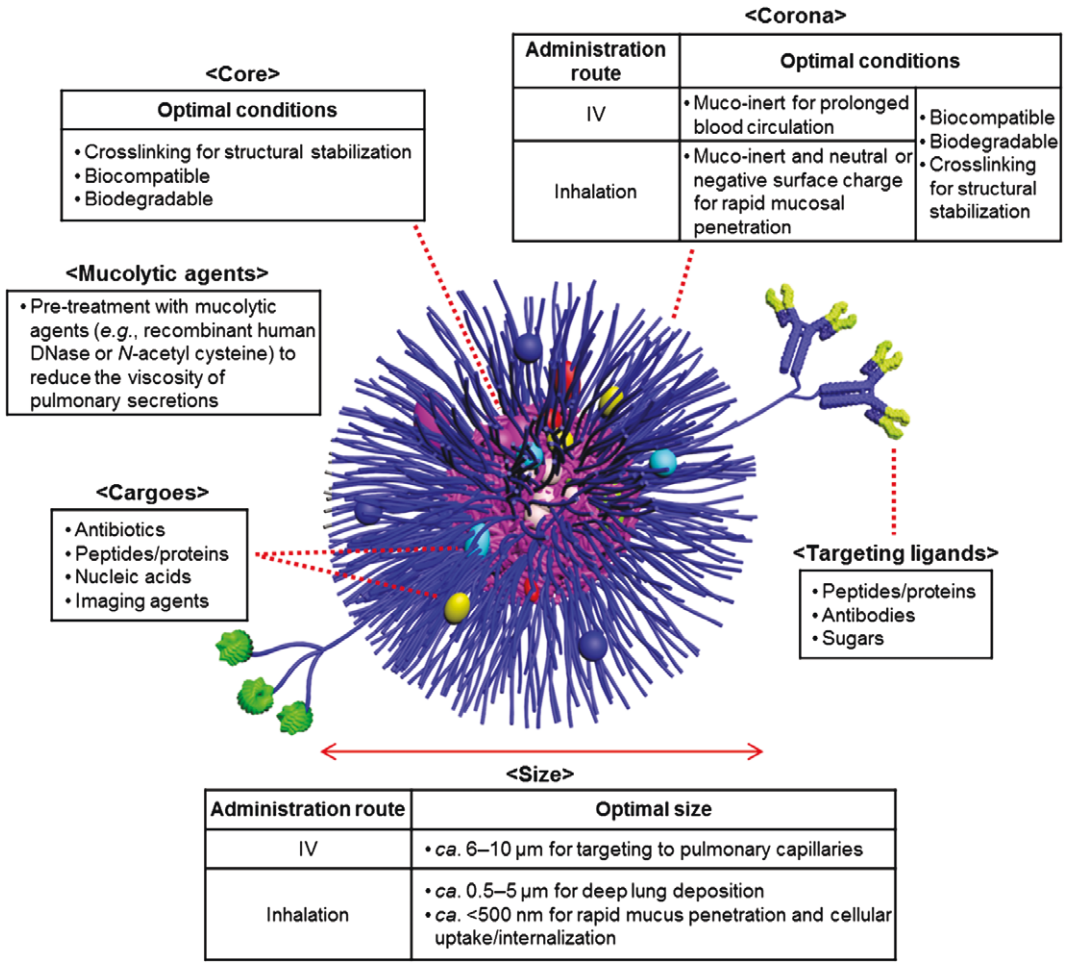

FIGURE 2 | Rational design of multifunctional polymeric NPs as delivery carriers for intravenous or pulmonary administration based on the published/introduced data.

Size

In the rational design of drug carriers for pulmonary delivery, there are several conflicting requirements for optimal d_{aer} of particles: (a) between ca. 500 nm and 5 μm to achieve deep lung deposition, (b) < ca. 500 nm or > ca. 6 μm and hydrophilic surface chemistry to avoid rapid clearance by alveolar macrophages, and (c) < ca. 200 nm for efficient mucus penetration and intracellular drug delivery.[16,26,33,137] To meet these conflicting restrictions on d_{aer}, nanometer-sized particles have been assembled in micrometer-sized aggregates.[77]

Once deposited in the lungs, transport of polymeric NPs is strongly dependent on the particle size and surface charge. NPs should be sufficiently smaller than ca. 200 nm, and coated with low MW stealth-like polymer chains, to overcome steric hindrance dictated by the mucus pores and the particulate interactions with the respiratory mucus contents.[83,86] However, cationic NPs of size smaller than ca. 34 nm showed lower transepithelial translocation from the lung than zwitterionic, anionic, and neutral NPs.[74,110]

Target/Binding Specificity

Introducing a mechanism to mediate a target-specific binding and/or triggered-drug release at the disease sites would enhance therapeutic efficacy while minimizing systemic side effects on normal tissues.[146,147] Although enhanced lung delivery by immuno-targeting the pulmonary endothelium with antibodies has been demonstrated following IV treatment,[148–152] the role of biomacromolecules as auxiliary devices for localized NP delivery via

inhalation administration for treatment of pulmonary infections remains poorly understood.

Meanwhile, enhanced uptake of NP formulations by alveolar macrophages, which express mannose receptors, could be realized by modifying the particle surface with mannose.[153] Chono et al. reported enhanced targeting efficiency to rat alveolar macrophages following pulmonary administration of mannosylated liposomes with 4-aminophenyl-*a*-D-mannopyranoside, which could be useful for the treatment of respiratory intracellular parasitic infections.[154]

Shape

Particles with various morphologies and/or aspect ratios may have different therapeutic loading capacities, *in vivo* fate, and toxicity. There is currently great effort to study the effect of particle shape and dimensions on cellular internalization and intracellular tracking, and phagocytosis both *in vitro* and *in vivo*, led particularly by DeSimone et al. and Mitragotri et al.[39,43,73,155–157] Recent studies by DeSimone et al. demonstrated noninflammatory response, homogenous lung distribution, increased lung residence time, and/or size-dependent macrophage uptake of donut and cylinder hydrogels in varying sizes upon instillation into the lungs of mice.[70,71] These results suggest that careful design and control over physical parameters of polymeric NPs will optimize their effective delivery of therapeutics to the lungs.

Surface Characteristics of NPs

Because of the presence of highly branched and negatively charged mucus glycoproteins of CF sputum overlying epithelial cells in the conductive airways and the higher tendency to provoke pulmonary inflammation by positively-charged polymeric NPs, it is generally accepted that the anionic or neutral surface characteristics of particulates would be optimal for pulmonary administration.[158] In particular, coating of NPs with inert polymers such as PEG showed promising results in penetrating into the highly viscoelastic human mucus secretions, minimizing adhesive interactions of NPs with mucus and protecting them against clearance by alveolar macrophages.[25,26]

Pre-Treatment of Mucus with Mucolytic Agents

Beyond modifying the surface chemistry of NPs, addition of mucolytic agents (e.g., rhDNase or NAC) can improve the mucus penetration of polymeric NPs by decreasing the mucus viscosity.[159] Examples included a ca. 3-fold improvement in the diffusion of NPs across the mucus upon addition of rhDNase demonstrated by De Smedt et al.,[63] ca. 13-fold increase in NP diffusion velocity in the presence of NAC showed by Hanes et al.,[96] formation of more homogeneous mucus pores leading to uniform NP diffusion velocities upon addition of rhDNase as highlighted by Hanes et al,[64] and improved penetration of DNase-functionalized NPs into CF sputum by Scott et al.[160] Careful selection of mucolytic agents is required because of possible inhibition of other mucolytics in combined pre-treatment strategies.[161]

Degradability of NPs

To address the concerns about immunotoxicity and long-term accumulation, use of biodegradable polymeric NP formulations is of critical importance,[16,162] as evidenced by reduced inflammation in the murine lung after intratracheal instillation of PLGA-based NPs of ca. 75 and 220 nm in diameter as compared to the PS-based nonbiodegradable counterparts of comparable size by Kissel et al.[162] Among other studies, CS- or PVA-modified PLGA NPs also did not show significant cytotoxicity to cultured lung epithelial cells.[115,163]

Despite extensive use of PLGA formulation in the inhaled delivery of therapeutics due to its biodegradability and biocompatibility, several factors, including its acidic degradation products, relatively slow hydrolysis rates, absence of functional moieties, and high degree of hydrophobicity, are detrimental for its use in pulmonary drug delivery.[114,164] Faster degradation rate of the PLGA component could be accomplished by preparing hydrophilic derivatives of PLGA, whereby increasing water saturation within the particles would promote hydrolytic degradation.[113,165,166]

An alternative aerosolized particle system of degradable polymer, polyketals, producing nonacidic degradation products upon hydrolysis was developed as a pulmonary delivery method by Baker et al.[167] Even though the polyketal-based particles were micron-sized (ca. 1.5—2.5 μm in diameter), they displayed no detectable alveolar or airway inflammation upon intratracheal instillation. Other classes of degradable NPs developed for pulmonary drug delivery include poly(ether-anhydrides),[168,169] polyphosphoesters,[122,123] polycarbonates, etc., and more comprehensive functional and toxicological studies are still needed with these systems.

Concluding Remarks

Polymeric NPs have been developed as effective carriers for delivery of various therapeutics and/or diagnostics for management of pulmonary infections due to their abilities to overcome drug resistance and to improve pharmacokinetics and biodistribution profiles of the administered drugs, thereby maximizing direct delivery and retention at the sites of infection while minimizing systemic exposure. Smart features also enable NPs to selectively release the loaded cargoes in specific microenvironments, disease sites, or other target sites in the body. However, there remain several challenges in the development of clinical nanomedicines for treatment of lung infections, including those associated with the conditions experienced during circulation and/or upon reaching the lung environment. For example, Dawson et al. raised concern over possible loss of the intended targeting capability of functionalized NPs in a biological environment.[170] In this study, the uptake of fluorescent silica NPs (SiO_2-PEG) conjugated with human transferrin (Tf), a transferrin receptor (TfR)-binding glycoprotein, in different types of serum was evaluated. The presence of fetal bovine serum reduced both the TfR-nonspecific and specific uptakes, demonstrating the total loss of TfR target specificity, depending on the type of serum. The authors postulated that this diminished target specificity of Tf-conjugated NPs arose from interactions with other proteins in the medium and the formation of a protein corona. This work highlights the significance of careful evaluation of the recognition, interactions and fates of bioconjugated NPs in a complex biological milieu. Recognition of the presence of a protein corona has become more prevalent, with significant enhancements in studies and techniques to evaluate the stability of synthetic NPs in the presence of biological macromolecules, including the kinetics and thermodynamics of the formation and dynamic remodeling of protein corona.[171–175] There is much effort to minimize non-specific interactions with biological macromolecules while promoting selective binding to receptors, the content of which has formed the basis of entirely separate review articles.[28,146,176–178]

In addition, promising results upon *in vitro* treatment in cell culture or *in vivo* administration in animal models may not guarantee the same outcomes in clinical trials. Hence, *in vitro* characterization data such as cytotoxicity, sputum penetration, and cellular uptake of medicated NPs should be validated with *in vivo* experiments for initial evidence that they can be tested under clinical settings. Although NPs have demonstrated significant potential in the treatment of lung infectious diseases, our current understanding of the complex interactions of the polymeric nanotherapeutics and the human body remains incomplete. Finally, lessons learned in the development of pulmonary NPs can be increasingly applied to NP administration at other epithelial sites, such as the gut, skin, and urinary tract. Such local administration is conceptually attractive due to diminished systemic effects of therapy, but each of these epithelial sites carries specific considerations for NP delivery optimization, such as mucus layers, immune cell populations, and other interacting moieties. Continued investigation at these various epithelial interfaces will inform the development of NP-based local therapies for common infections as well as for other epithelial diseases.

ACKNOWLEDGMENTS

We gratefully acknowledge financial support from the National Heart Lung and Blood Institute of the National Institutes of Health as a Program of Excellence in Nanotechnology (HHSN268201000046C), the National Institute of Diabetes and Digestive and Kidney Diseases of the National Institutes of Health (R01-DK082546 and P50-DK064540), and the National Science Foundation (DMR-1507429 and CHE-1410272). The Welch Foundation is gratefully acknowledged for support through the W. T. Doherty-Welch Chair in Chemistry, Grant No. A-0001. Financial support from the Egyptian Ministry of Scientific Research – Science and Technology Development Fund (Demand-driven Project 5688 and Reintegration Grant 5362), and the Ministry of Higher Education (CEP2-007-ASSU) are gratefully acknowledged (M.E.).

REFERENCES

1. Allen TM, Cullis PR. Drug delivery systems: entering the mainstream. *Science* 2004, 303:1818–1822. doi:10.1126/science.1095833.
2. Koul A, Arnoult E, Lounis N, Guillemont J, Andries K. The challenge of new drug discovery for tuberculosis. *Nature* 2011, 469:483–490. doi:10.1038/nature09657.

3. Zhang L, Gu FX, Chan JM, Wang AZ, Langer RS, Farokhzad OC. Nanoparticles in medicine: therapeutic applications and developments. *Clin Pharmacol Ther* 2008, 83:761–769. doi:10.1038/sj.clpt.6100400.
4. Wagner V, Dullaart A, Bock AK, Zweck A. The emerging nanomedicine landscape. *Nat Biotechnol* 2006, 24:1211–1217. doi:10.1038/nbt1006-1211.
5. Zhao F, Zhao Y, Liu Y, Chang X, Chen C. Cellular uptake, intracellular trafficking, and cytotoxicity of nanomaterials. *Small* 2011, 7:1322–1337. doi:10.1002/smll.201100001.
6. Veiseh O, Gunn JW, Zhang M. Design and fabrication of magnetic nanoparticles for targeted drug delivery and imaging. *Adv Drug Deliv Rev* 2010, 62:284–304. doi:10.1016/j.addr.2009.11.002.
7. Elsabahy M, Wooley KL. Strategies toward well-defined polymer nanoparticles inspired by nature: chemistry versus versatility. *J Polym Sci A Polym Chem* 2012, 50:1869–1880. doi:10.1002/pola.25955.
8. Patton JS, Byron PR. Inhaling medicines: delivering drugs to the body through the lungs. *Nat Rev Drug Discov* 2007, 6:67–74. doi:10.1038/nrd2153.
9. Rosen H, Abribat T. The rise and rise of drug delivery. *Nat Rev Drug Discov* 2005, 4:381–385. doi:10.1038/nrd1721.
10. Marco MD, Shamsuddin S, Razak KA, Aziz AA, Devaux C, Borghi E, Levy L, Sadun C. Overview of the main methods used to combine proteins with nanosystems: absorption, bioconjugation, and encapsulation. *Int J Nanomedicine* 2010, 5:37–49. doi:10.2147/ijn.S6458.
11. Roger E, Lagarce F, Garcion E, Benoit JP. Biopharmaceutical parameters to consider in order to alter the fate of nanocarriers after oral delivery. *Nanomedicine* 2010, 5:287–306. doi:10.2217/nnm.09.110.
12. Chao P, Deshmukh M, Kutscher HL, Gao D, Rajan SS, Hu P, Laskin DL, Stein S, Sinko PJ. Pulmonary targeting microparticulate camptothecin delivery system: anticancer evaluation in a rat orthotopic lung cancer model. *Anticancer Drugs* 2010, 21:65–76. doi:10.1097/cad.0b013e328332a322.
13. Koster VS, Kuks PFM, Lange R, Talsma H. Particle size in parenteral fat emulsions, what are the true limitations? *Int J Pharm* 1996, 134:235–238. doi:10.1016/0378-5173(95)04409-4.
14. Andrade F, Videira M, Ferreira D, Sarmento B. Nanocarriers for pulmonary administration of peptides and therapeutic proteins. *Nanomedicine* 2011, 6:123–141. doi:10.2217/nnm.10.143.
15. Bur M, Henning A, Hein S, Schneider M, Lehr C-M. Inhalative nanomedicine—opportunities and challenges. *Inhal Toxicol* 2009, 21(Suppl 1):137–143. doi:10.1080/08958370902962283.
16. Sung JC, Pulliam BL, Edwards DA. Nanoparticles for drug delivery to the lungs. *Trends Biotechnol* 2007, 25:563–570. doi:10.1016/j.tibtech.2007.09.005.
17. Patton JS, Fishburn CS, Weers JG. The lungs as a portal of entry for systemic drug delivery. *Proc Am Thorac Soc* 2004, 1:338–344. doi:10.1513/pats.200409-049TA.
18. Meers P, Neville M, Malinin V, Scotto AW, Sardaryan G, Kurumunda R, Mackinson C, James G, Fisher S, Perkins WR. Biofilm penetration, triggered release and in vivo activity of inhaled liposomal amikacin in chronic pseudomonas aeruginosa lung infections. *J Antimicrob Chemother* 2008, 61:859–868. doi:10.1093/jac/dkn059.
19. Dailey LA, Schmehl T, Gessler T, Wittmar M, Grimminger F, Seeger W, Kissel T. Nebulization of biodegradable nanoparticles: impact of nebulizer technology and nanoparticle characteristics on aerosol features. *J Control Release* 2003, 86:131–144. doi:10.1016/S0168-3659(02)00370-X.
20. Courrier HM, Butz N, Vandamme TF. Pulmonary drug delivery systems: recent developments and prospects. *Crit Rev Ther Drug Carr Syst* 2002, 19:425–498. doi:10.1615/CritRevTherDrugCarrierSyst.v19.i45.40.
21. Azarmi S, Roa WH, Löbenberg R. Targeted delivery of nanoparticles for the treatment of lung diseases. *Adv Drug Deliv Rev* 2008, 60:863–875. doi:10.1016/j.addr.2007.11.006.
22. Omlor A, Nguyen J, Bals R, Dinh QT. Nanotechnology in respiratory medicine. *Respir Res* 2015, 16:64. doi:10.1186/s12931-015-0223-5.
23. Kobayashi K, Wei J, Iida R, Ijiro K, Niikura K. Surface engineering of nanoparticles for therapeutic applications. *Polym J* 2014, 46:460–468. doi:10.1038/pj.2014.40.
24. Elsabahy M, Wooley K. Design of polymeric nanoparticles for biomedical delivery applications. *Chem Soc Rev* 2012, 41:2545–2561. doi:10.1039/c2cs15327k.
25. Sanders N, Rudolph C, Braeckmans K, De Smedt SC, Demeester J. Extracellular barriers in respiratory gene therapy. *Adv Drug Deliv Rev* 2009, 61:115–127. doi:10.1016/j.addr.2008.09.011.
26. Lai SK, Wang Y-Y, Hanes J. Mucus-penetrating nanoparticles for drug and gene delivery to mucosal tissues. *Adv Drug Deliv Rev* 2009, 61:158–171. doi:10.1016/j.addr.2008.11.002.
27. Lai SK, Wang YY, Wirtz D, Hanes J. Micro- and macrorheology of mucus. *Adv Drug Deliv Rev* 2009, 61:86–100. doi:10.1016/j.addr.2008.09.012.
28. Petros R, DeSimone J. Strategies in the design of nanoparticles for therapeutic applications. *Nat Rev Drug Discov* 2010, 9:615–627. doi:10.1038/nrd2591.

29. Dobrovolskaia MA, McNeil SE. Immunological properties of engineered nanomaterials. *Nat Nanotechnol* 2007, 2:469–478. doi:10.1038/nnano.2007.223.
30. Lee WH, Loo CY, Traini D, Young PM. Nano- and micro-based inhaled drug delivery systems for targeting alveolar macrophages. *Expert Opin Drug Deliv* 2015, 12:1009–1026. doi:10.1517/17425247.2015.1039509.
31. Griffiths G, Nystroem B, Sable SB, Khuller GK. Nanobead-based interventions for the treatment and prevention of tuberculosis. *Nat Rev Microbiol* 2010, 8:827–834. doi:10.1038/nrmicro2437.
32. Elsabahy M, Wooley KL. Cytokines as biomarkers of nanoparticle immunotoxicity. *Chem Soc Rev* 2013, 42:5552–5576. doi:10.1039/c3cs60064e.
33. Champion J, Walker A, Mitragotri S. Role of particle size in phagocytosis of polymeric microspheres. *Pharm Res* 2008, 25:1815–1821. doi:10.1007/s11095-008-9562-y.
34. Jiang W, Kim BYS, Rutka JT, Chan WCW. Nanoparticle-mediated cellular response is size-dependent. *Nat Nanotechnol* 2008, 3:145–150. doi:10.1038/nnano.2008.30.
35. Rejman J, Oberle V, Zuhorn IS, Hoekstra D. Size-dependent internalization of particles via the pathways of clathrin-and caveolae-mediated endocytosis. *Biochem J* 2004, 377:159–169. doi:10.1042/bj20031253.
36. Hirn S, Semmler-Behnke M, Schleh C, Wenk A, Lipka J, Schaffler M, Takenaka S, Moller W, Schmid G, Simon U, et al. Particle size-dependent and surface charge-dependent biodistribution of gold nanoparticles after intravenous administration. *Eur J Pharm Biopharm* 2011, 77:407–416. doi:10.1016/j.ejpb.2010.12.029.
37. Champion JA, Katare YK, Mitragotri S. Particle shape: a new design parameter for micro- and nanoscale drug delivery carriers. *J Control Release* 2007, 121:3–9. doi:10.1016/j.jconrel.2007.03.022.
38. Geng Y, Dalhaimer P, Cai S, Tsai R, Tewari M, Minko T, Discher DE. Shape effects of filaments versus spherical particles in flow and drug delivery. *Nat Nanotechnol* 2007, 2:249–255. doi:10.1038/nnao.2007.70.
39. Champion JA, Mitragotri S. Role of target geometry in phagocytosis. *Proc Natl Acad Sci USA* 2006, 103:4930–4934. doi:10.1073/pnas.0600997103.
40. Gessner A, Lieske A, Paulke BR, Müller RH. Influence of surface charge density on protein adsorption on polymeric nanoparticles: analysis by two-dimensional electrophoresis. *Eur J Pharm Biopharm* 2002, 54:165–170. doi:10.1016/S0939-6411(02)00081-4.
41. Gessner A, Waicz R, Lieske A, Paulke BR, Mäder K, Müller RH. Nanoparticles with decreasing surface hydrophobicities: influence on plasma protein adsorption. *Int J Pharm* 2000, 196:245–249. doi:10.1016/S0378-5173(99)00432-9.
42. Card JW, Zeldin DC, Bonner JC, Nestmann ER. Pulmonary applications and toxicity of engineered nanoparticles. *Am J Physiol Lung Cell Mol Physiol* 2008, 295:L400–L411. doi:10.1152/ajplung.00041.2008.
43. Gratton SEA, Ropp PA, Pohlhaus PD, Luft JC, Madden VJ, Napier ME, DeSimone JM. The effect of particle design on cellular internalization pathways. *Proc Natl Acad Sci USA* 2008, 105:11613–11618. doi:10.1073/pnas.0801763105.
44. Mitragotri S, Lahann J. Physical approaches to biomaterial design. *Nat Mater* 2009, 8:15–23. doi:10.1038/nmat2344.
45. Chow AHL, Tong HHY, Chattopadhyay P, Shekunov BY. Particle engineering for pulmonary drug delivery. *Pharm Res* 2007, 24:411–437. doi:10.1007/s11095-006-9174-3.
46. Alexis F, Pridgen E, Molnar LK, Farokhzad OC. Factors affecting the clearance and biodistribution of polymeric nanoparticles. *Mol Pharm* 2008, 5:505–515. doi:10.1021/mp800051m.
47. Elsabahy M, Zhang S, Zhang F, Deng ZJ, Lim YH, Wang H, Parsamian P, Hammond PT, Wooley KL. Surface charges and shell crosslinks each play significant roles in mediating degradation, biofouling, cytotoxicity and immunotoxicity for polyphosphoester-based nanoparticles. *Sci Rep* 2013, 3. doi:10.1038/srep03313.
48. Decuzzi P, Godin B, Tanaka T, Lee SY, Chiappini C, Liu X, Ferrari M. Size and shape effects in the biodistribution of intravascularly injected particles. *J Control Release* 2010, 141:320–327. doi:10.1016/j.jconrel.2009.10.014.
49. Ilium L, Davis SS, Wilson CG, Thomas NW, Frier M, Hardy JG. Blood clearance and organ deposition of intravenously administered colloidal particles. the effects of particle size, nature and shape. *Int J Pharm* 1982, 12:135–146. doi:10.1016/0378-5173(82)90113-2.
50. Kutscher HL, Chao P, Deshmukh M, Singh Y, Hu P, Joseph LB, Reimer DC, Stein S, Laskin DL, Sinko PJ. Threshold size for optimal passive pulmonary targeting and retention of rigid microparticles in rats. *J Control Release* 2010, 143:31–37. doi:10.1016/j.jconrel.2009.12.019.
51. Gao H, Xiong J, Cheng T, Liu J, Chu L, Ma R, Shi L. In vivo biodistribution of mixed shell micelles with tunable hydrophilic/hydrophobic surface. *Biomacromolecules* 2013, 14:460–467. doi:10.1021/bm301694t.
52. Sheng Y, Liu C, Yuan Y, Tao X, Yang F, Shan X, Zhou H, Xu F. Long-circulating polymeric nanoparticles bearing a combinatorial coating of PEG and water-soluble chitosan.

Biomaterials 2009, 30:2340–2348. doi:10.1016/j.biomaterials.2008.12.070.

53. Sasatsu M, Onishi H, Machida Y. Preparation and biodisposition of methoxypolyethylene glycol amine-poly(dl-lactic acid) copolymer nanoparticles loaded with pyrene-ended poly(dl-lactic acid). *Int J Pharm* 2008, 358:271–277. doi:10.1016/j.ijpharm.2008.03.011.
54. Sarlo K, Blackburn KL, Clark ED, Grothaus J, Chaney J, Neu S, Flood J, Abbott D, Bohne C, Casey K, et al. Tissue distribution of 20 nm, 100 nm and 1000 nm fluorescent polystyrene latex nanospheres following acute systemic or acute and repeat airway exposure in the rat. *Toxicology* 2009, 263:117–126. doi:10.1016/j.tox.2009.07.002.
55. Simon BH, Ando HY, Gupta PK. Circulation time and body distribution of 14C-labeled amino-modified polystyrene nanoparticles in mice. *J Pharm Sci* 1995, 84:1249–1253. doi:10.1002/jps.2600841020.
56. Deshmukh M, Kutscher HL, Gao D, Sunil VR, Malaviya R, Vayas K, Stein S, Laskin JD, Laskin DL, Sinko PJ. Biodistribution and renal clearance of biocompatible lung targeted poly(ethylene glycol) (PEG) nanogel aggregates. *J Control Release* 2012, 164:65–73. doi:10.1016/j.jconrel.2012.09.011.
57. Pinkerton NM, Zhang SW, Youngblood RL, Gao D, Li S, Benson BR, Anthony J, Stone HA, Sinko PJ, Prud'homme RK. Gelation chemistries for the encapsulation of nanoparticles in composite gel microparticles for lung imaging and drug delivery. *Biomacromolecules* 2013, 15:252–261. doi:10.1021/bm4015232.
58. Loira-Pastoriza C, Todoroff J, Vanbever R. Delivery strategies for sustained drug release in the lungs. *Adv Drug Deliv Rev* 2014, 75:81–91. doi:10.1016/j.addr.2014.05.017.
59. Son Y-J, McConville JT. Advancements in dry powder delivery to the lung. *Drug Dev Ind Pharm* 2008, 34:948–959. doi:10.1080/03639040802235902.
60. Bailey MM, Berkland CJ. Nanoparticle formulations in pulmonary drug delivery. *Med Res Rev* 2009, 29:196–212. doi:10.1002/med.20140.
61. Zhang J, Wu L, Chan HK, Watanabe W. Formation, characterization, and fate of inhaled drug nanoparticles. *Adv Drug Deliv Rev* 2011, 63:441–455. doi:10.1016/j.addr.2010.11.002.
62. Rubin BK, Williams RW. Emerging aerosol drug delivery strategies: From bench to clinic. *Adv Drug Deliv Rev* 2014, 75:141–148. doi:10.1016/j.addr.2014.06.008.
63. Sanders NN, De Smedt SC, Van Rompaey E, Simoens P, De Baets F, Demeester J. Cystic fibrosis sputum: a barrier to the transport of nanospheres. *Am J Respir Crit Care Med* 2000, 162:1905–1911. doi:10.1164/ajrccm.162.5.9909009.
64. Dawson M, Wirtz D, Hanes J. Enhanced viscoelasticity of human cystic fibrotic sputum correlates with increasing microheterogeneity in particle transport. *J Biol Chem* 2003, 278:50393–50401. doi:10.1074/jbc.m309026200.
65. Ensign LM, Henning A, Schneider CS, Maisel K, Wang YY, Porosoff MD, Cone R, Hanes J. Ex vivo characterization of particle transport in mucus secretions coating freshly excised mucosal tissues. *Mol Pharm* 2013, 10:2176–2182. doi:10.1021/mp400087y.
66. Kirch J, Guenther M, Doshi N, Schaefer UF, Schneider M, Mitragotri S, Lehr CM. Mucociliary clearance of micro- and nanoparticles is independent of size, shape and charge-an ex vivo and in silico approach. *J Control Release* 2012, 159:128–134. doi:10.1016/j.jconrel.2011.12.015.
67. Henning A, Schneider M, Nafee N, Muijs L, Rytting E, Wang XY, Kissel T, Grafahrend D, Klee D, Lehr CM. Influence of particle size and material properties on mucociliary clearance from the airways. *J Aerosol Med Pulm Drug Deliv* 2010, 23:233–241. doi:10.1089/jamp.2009.0806.
68. Liu Y, Ibricevic A, Cohen JA, Cohen JL, Gunsten SP, Fréchet JMJ, Walter MJ, Welch MJ, Brody SL. Impact of hydrogel nanoparticle size and functionalization on in vivo behavior for lung imaging and therapeutics. *Mol Pharm* 2009, 6:1891–1902. doi:10.1021/mp900215p.
69. Makino K, Yamamoto N, Higuchi K, Harada N, Ohshima H, Terada H. Phagocytic uptake of polystyrene microspheres by alveolar macrophages: effects of the size and surface properties of the microspheres. *Colloids Surf B* 2003, 27:33–39. doi:10.1016/S0927-7765(02)00042-5.
70. Roberts RA, Shen T, Allen IC, Hasan W, DeSimone JM, Ting JPY. Analysis of the murine immune response to pulmonary delivery of precisely fabricated nano- and microscale particles. *PLoS One* 2013, 8:e62115. doi:10.1371/journal.pone.0062115.
71. Shen TW, Fromen CA, Kai MP, Luft JC, Rahhal TB, Robbins GR, DeSimone JM. Distribution and cellular uptake of PEGylated polymeric particles in the lung towards cell-specific targeted delivery. *Pharm Res* 2015, 32:3248–3260. doi:10.1007/s11095-015-1701-7.
72. Doshi N, Mitragotri S. Macrophages recognize size and shape of their targets. *PLoS One* 2010, 5:e10051. doi:10.1371/journal.pone.0010051.
73. Sharma G, Valenta DT, Altman Y, Harvey S, Xie H, Mitragotri S, Smith JW. Polymer particle shape independently influences binding and internalization by macrophages. *J Control Release* 2010, 147:408–412. doi:10.1016/j.jconrel.2010.07.116.
74. Choi HS, Ashitate Y, Lee JH, Kim SH, Matsui A, Insin N, Bawendi MG, Semmler-Behnke M,

Frangioni JV, Tsuda A. Rapid translocation of nanoparticles from the lung airspaces to the body. *Nat Biotechnol* 2010, 28:1300–1303. doi:10.1038/nbt.1696.

75. Kreyling WG, Hirn S, Schleh C. Nanoparticles in the lung. *Nat Biotechnol* 2010, 28:1275–1276. doi:10.1038/nbt.1735.
76. Mohammad AK, Amayreh LK, Mazzara JM, Reineke JJ. Rapid lymph accumulation of polystyrene nanoparticles following pulmonary administration. *Pharm Res* 2013, 30:424–434. doi:10.1007/s11095-012-0884-4.
77. Ungaro F, d'Angelo I, Coletta C, d'Emmanuele di Villa Bianca R, Sorrentino R, Perfetto B, Tufano MA, Miro A, La Rotonda MI, Quaglia F. Dry powders based on PLGA nanoparticles for pulmonary delivery of antibiotics: modulation of encapsulation efficiency, release rate and lung deposition pattern by hydrophilic polymers. *J Control Release* 2012, 157:149–159. doi:10.1016/j.jconrel.2011.08.010.
78. Yang M, Lai SK, Yu T, Wang YY, Happe C, Zhong WX, Zhang M, Anonuevo A, Fridley C, Hung A, et al. Nanoparticle penetration of human cervicovaginal mucus: the effect of polyvinyl alcohol. *J Control Release* 2014, 192:202–208. doi:10.1016/j.jconrel.2014.07.045.
79. Forier K, Messiaen AS, Raemdonck K, Deschout H, Rejman J, De Baets F, Nelis H, De Smedt SC, Demeester J, Coenye T, et al. Transport of nanoparticles in cystic fibrosis sputum and bacterial biofilms by single-particle tracking microscopy. *Nanomedicine* 2013, 8:935–949. doi:10.2217/nnm.12.129.
80. Chen EYT, Wang YC, Chen CS, Chin WC. Functionalized positive nanoparticles reduce mucin swelling and dispersion. *PLoS One* 2010, 5:e15434. doi:10.1371/journal.pone.0015434.
81. Jokerst JV, Lobovkina T, Zare RN, Gambhir SS. Nanoparticle PEGylation for imaging and therapy. *Nanomedicine* 2011, 6:715–728. doi:10.2217/nnm.11.19.
82. Boylan NJ, Kim AJ, Suk JS, Adstamongkonkul P, Simons BW, Lai SK, Cooper MJ, Hanes J. Enhancement of airway gene transfer by DNA nanoparticles using a pH-responsive block copolymer of polyethylene glycol and poly-L-lysine. *Biomaterials* 2012, 33:2361–2371. doi:10.1016/j.biomaterials.2011.11.080.
83. Schuster BS, Suk JS, Woodworth GF, Hanes J. Nanoparticle diffusion in respiratory mucus from humans without lung disease. *Biomaterials* 2013, 34:3439–3446. doi:10.1016/j.biomaterials.2013.01.064.
84. Tang BC, Dawson M, Lai SK, Wang YY, Suk JS, Yang M, Zeitlin P, Boyle MP, Fu J, Hanes J. Biodegradable polymer nanoparticles that rapidly penetrate the human mucus barrier. *Proc Natl Acad Sci USA* 2009, 106:19268–19273. doi:10.1073/pnas.0905998106.
85. Lai SK, O'Hanlon DE, Harrold S, Man ST, Wang Y-Y, Cone R, Hanes J. Rapid transport of large polymeric nanoparticles in fresh undiluted human mucus. *Proc Natl Acad Sci USA* 2007, 104:1482–1487. doi:10.1073/pnas.0608611104.
86. Suk JS, Lai SK, Wang YY, Ensign LM, Zeitlin PL, Boyle MP, Hanes J. The penetration of fresh undiluted sputum expectorated by cystic fibrosis patients by non-adhesive polymer nanoparticles. *Biomaterials* 2009, 30:2591–2597. doi:10.1016/j.biomaterials.2008.12.076.
87. Wang YY, Lai SK, Suk JS, Pace A, Cone R, Hanes J. Addressing the PEG mucoadhesivity paradox to engineer nanoparticles that "slip" through the human mucus barrier. *Angew Chem Int Ed* 2008, 47:9726–9729. doi:10.1002/anie.200803526.
88. Suk JS, Kim AJ, Trehan K, Schneider CS, Cebotaru L, Woodward OM, Boylan NJ, Boyle MP, Lai SK, Guggino WB, et al. Lung gene therapy with highly compacted DNA nanoparticles that overcome the mucus barrier. *J Control Release* 2014, 178:8–17. doi:10.1016/j.jconrel.2014.01.007.
89. Kleemann E, Jekel N, Dailey LA, Roesler S, Fink L, Weissmann N, Schermuly R, Gessler T, Schmehl T, Roberts CJ, et al. Enhanced gene expression and reduced toxicity in mice using polyplexes of low-molecular-weight poly(ethylene imine) for pulmonary gene delivery. *J Drug Target* 2009, 17:638–651. doi:10.1080/10611860903106414.
90. Cu Y, Saltzman WM. Controlled surface modification with poly(ethylene)glycol enhances diffusion of PLGA nanoparticles in human cervical mucus. *Mol Pharm* 2009, 6:173–181. doi:10.1021/mp8001254.
91. Boylan NJ, Suk JS, Lai SK, Jelinek R, Boyle MP, Cooper MJ, Hanes J. Highly compacted DNA nanoparticles with low MW PEG coatings: in vitro, ex vivo and in vivo evaluation. *J Control Release* 2012, 157:72–79. doi:10.1016/j.jconrel.2011.08.031.
92. Ishida T, Ichihara M, Wang X, Yamamoto K, Kimura J, Majima E, Kiwada H. Injection of PEGylated liposomes in rats elicits PEG-specific IgM, which is responsible for rapid elimination of a second dose of PEGylated liposomes. *J Control Release* 2006, 112:15–25. doi:10.1016/j.jconrel.2006.01.005.
93. Otsuka H, Nagasaki Y, Kataoka K. PEGylated nanoparticles for biological and pharmaceutical applications. *Adv Drug Deliv Rev* 2012, 64:246–255. doi:10.1016/j.addr.2012.09.022.
94. Gallon AM. Evaluation of nebulised acetylcysteine and normal saline in the treatment of sputum retention following thoracotomy. *Thorax* 1996, 51:429–432. doi:10.1136/thx.51.4.429.

95. Henke MO, Ratjen F. Mucolytics in cystic fibrosis. *Paediatr Respir Rev* 2007, 8:24–29. doi:10.1016/j.prrv.2007.02.009.

96. Suk JS, Lai SK, Boylan NJ, Dawson MR, Boyle MP, Hanes J. Rapid transport of muco-inert nanoparticles in cystic fibrosis sputum treated with N-acetyl cysteine. *Nanomedicine* 2011, 6:365–375. doi:10.2217/nnm.10.123.

97. Suk JS, Boylan NJ, Trehan K, Tang BC, Schneider CS, Lin JMG, Boyle MP, Zeitlin PL, Lai SK, Cooper MJ, et al. N-acetylcysteine enhances cystic fibrosis sputum penetration and airway gene transfer by highly compacted DNA nanoparticles. *Mol Ther* 2011, 19:1981–1989. doi:10.1038/mt.2011.160.

98. Schuster BS, Kim AJ, Kays JC, Kanzawa MM, Guggino WB, Boyle MP, Rowe SM, Muzyczka N, Suk JS, Hanes J. Overcoming the cystic fibrosis sputum barrier to leading adeno-associated virus gene therapy vectors. *Mol Ther* 2014, 22:1484–1493. doi:10.1038/mt.2014.89.

99. Mehanna MM, Mohyeldin SM, Elgindy NA. Respirable nanocarriers as a promising strategy for antitubercular drug delivery. *J Control Release* 2014, 187:183–197. doi:10.1016/j.jconrel.2014.05.038.

100. Zhang F, Zhang S, Pollack SF, Li R, Gonzalez AM, Fan J, Zou J, Leininger SE, Pavía-Sanders A, Johnson R, et al. Improving paclitaxel delivery: in vitro and in vivo characterization of PEGylated polyphosphoester-based nanocarriers. *J Am Chem Soc* 2015, 137:2056–2066. doi:10.1021/ja512616s.

101. Aweda TA, Zhang S, Mupanomunda C, Burkemper J, Heo GS, Bandara N, Lin M, Cutler CS, Cannon CL, Youngs WJ, et al. Investigating the pharmacokinetics and biological distribution of silver-loaded polyphosphoester-based nanoparticles using 111Ag as a radiotracer. *J Labelled Comp Radiopharm* 2015, 58:234–241. doi:10.1002/jlcr.3289.

102. Shah PN, Lin LY, Smolen JA, Tagaev JA, Gunsten SP, Han DS, Heo GS, Li Y, Zhang F, Zhang S, et al. Synthesis, characterization, and in vivo efficacy of shell cross-linked nanoparticle formulations carrying silver antimicrobials as aerosolized therapeutics. *ACS Nano* 2013, 7:4977–4987. doi:10.1021/nn400322f.

103. Mura S, Hillaireau H, Nicolas J, Kerdine-Römer S, Le Droumaguet B, Delomènie C, Nicolas V, Pallardy M, Tsapis N, Fattal E. Biodegradable nanoparticles meet the bronchial airway barrier: how surface properties affect their interaction with mucus and epithelial cells. *Biomacromolecules* 2011, 12:4136–4143. doi:10.1021/bm201226x.

104. Menon JU, Ravikumar P, Pise A, Gyawali D, Hsia CCW, Nguyen KT. Polymeric nanoparticles for pulmonary protein and DNA delivery. *Acta Biomater* 2014, 10:2643–2652. doi:10.1016/j.actbio.2014.01.033.

105. Choi M, Cho M, Han BS, Hong J, Jeong J, Park S, Cho M-H, Kim K, Cho W-S. Chitosan nanoparticles show rapid extrapulmonary tissue distribution and excretion with mild pulmonary inflammation to mice. *Toxicol Lett* 2010, 199:144–152. doi:10.1016/j.toxlet.2010.08.016.

106. Hara K, Tsujimoto H, Tsukada Y, Huang CC, Kawashima Y, Tsutsumi M. Histological examination of PLGA nanospheres for intratracheal drug administration. *Int J Pharm* 2008, 356:267–273. doi:10.1016/j.ijpharm.2007.12.041.

107. Dombu CY, Kroubi M, Zibouche R, Matran R, Betbeder D. Characterization of endocytosis and exocytosis of cationic nanoparticles in airway epithelium cells. *Nanotechnology* 2010, 21:355102. doi:10.1088/0957-4484/21/35/355102.

108. Lai SK, Hida K, Man ST, Chen C, Machamer C, Schroer TA, Hanes J. Privileged delivery of polymer nanoparticles to the perinuclear region of live cells via a non-clathrin, non-degradative pathway. *Biomaterials* 2007, 28:2876–2884. doi:10.1016/j.biomaterials.2007.02.021.

109. Lühmann T, Rimann M, Bittermann AG, Hall H. Cellular uptake and intracellular pathways of PLL-g-PEG-DNA nanoparticles. *Bioconjugate Chem* 2008, 19:1907–1916. doi:10.1021/bc800206r.

110. Ibricevic A, Guntsen SP, Zhang K, Shrestha R, Liu Y, Sun JY, Welch MJ, Wooley KL, Brody SL. PEGylation of cationic, shell-crosslinked-knedel-like nanoparticles modulates inflammation and enhances cellular uptake in the lung. *Nanomedicine* 2013, 9:912–922. doi:10.1016/j.nano.2013.02.006.

111. Kim AJ, Boylan NJ, Suk JS, Lai SK, Hanes J. Non-degradative intracellular trafficking of highly compacted polymeric DNA nanoparticles. *J Control Release* 2012, 158:102–107. doi:10.1016/j.jconrel.2011.10.031.

112. Kemp SJ, Thorley AJ, Gorelik J, Seckl MJ, O'Hare MJ, Arcaro A, Korchev Y, Goldstraw P, Tetley TD. Immortalization of human alveolar epithelial cells to investigate nanoparticle uptake. *Am J Respir Cell Mol Biol* 2008, 39:591–597. doi:10.1165/rcmb.2007-0334oc.

113. Dailey LA, Kleemann E, Wittmar M, Gessler T, Schmehl T, Roberts C, Seeger W, Kissel T. Surfactant-free, biodegradable nanoparticles for aerosol therapy based on the branched polyesters, DEAPA-PVAL-g-PLGA. *Pharm Res* 2003, 20:2011–2020. doi:10.1023/b:pham.0000008051.94834.10.

114. Harush-Frenkel O, Bivas-Benita M, Nassar T, Springer C, Sherman Y, Avital A, Altschuler Y, Borlak J, Benita S. A safety and tolerability study of differently-charged nanoparticles for local pulmonary

drug delivery. *Toxicol Appl Pharm* 2010, 246:83–90. doi:10.1016/j.taap.2010.04.011.

115. Grabowski N, Hillaireau H, Vergnaud J, Santiago LA, Kerdine-Romer S, Pallardy M, Tsapis N, Fattal E. Toxicity of surface-modified PLGA nanoparticles toward lung alveolar epithelial cells. *Int J Pharm* 2013, 454:686–694. doi:10.1016/j.ijpharm.2013.05.025.

116. Jones MC, Jones SA, Riffo-Vasquez Y, Spina D, Hoffman E, Morgan A, Patel A, Page C, Forbes B, Dailey LA. Quantitative assessment of nanoparticle surface hydrophobicity and its influence on pulmonary biocompatibility. *J Control Release* 2014, 183:94–104. doi:10.1016/j.jconrel.2014.03.022.

117. Valle RP, Huang CL, Loo JSC, Zuo YY. Increasing hydrophobicity of nanoparticles intensifies lung surfactant film inhibition and particle retention. *ACS Sustain Chem Eng* 2014, 2:1574–1580. doi:10.1021/sc500100b.

118. Hindi KM, Ditto AJ, Panzner MJ, Medvetz DA, Han DS, Hovis CE, Hilliard JK, Taylor JB, Yun YH, Cannon CL, et al. The antimicrobial efficacy of sustained release silver–carbene complex-loaded l-tyrosine polyphosphate nanoparticles: characterization, in vitro and in vivo studies. *Biomaterials* 2009, 30:3771–3779. doi:10.1016/j.biomaterials.2009.03.044.

119. Kascatan Nebioglu A, Panzner M, Tessier C, Cannon C, Youngs W. N-heterocyclic carbene–silver complexes: a new class of antibiotics. *Coord Chem Rev* 2007, 251:884–895. doi:10.1016/j.ccr.2006.08.019.

120. Bjarnsholt T, Kirketerp-Moller K, Kristiansen S, Phipps R, Nielsen AK, Jensen PO, Hoiby N, Givskov M. Silver against Pseudomonas aeruginosa biofilms. *APMIS* 2007, 115:921–928. doi:10.1111/j.1600-0463.2007.apm_646.x.

121. Ornelas-Megiatto C, Shah PN, Wich PR, Cohen JL, Tagaev JA, Smolen JA, Wright BD, Panzner MJ, Youngs WJ, Fréchet JMJ, et al. Aerosolized antimicrobial agents based on degradable dextran nanoparticles loaded with silver carbene complexes. *Mol Pharm* 2012, 9:3012–3022. doi:10.1021/mp3004379.

122. Lim YH, Tiemann KM, Heo GS, Wagers PO, Rezenom YH, Zhang S, Zhang F, Youngs WJ, Hunstad DA, Wooley KL. Preparation and in vitro antimicrobial activity of silver-bearing degradable polymeric nanoparticles of polyphosphoester-block-poly(l-lactide). *ACS Nano* 2015, 9:1995–2008. doi:10.1021/nn507046h.

123. Zhang F, Smolen JA, Zhang S, Li R, Shah PN, Cho S, Wang H, Raymond JE, Cannon CL, Wooley KL. Degradable polyphosphoester-based silver-loaded nanoparticles as therapeutics for bacterial lung infections. *Nanoscale* 2015, 7:2265–2270. doi:10.1039/c4nr07103d.

124. Pandey R, Zahoor A, Sharma S, Khuller GK. Nanoparticle encapsulated antitubercular drugs as a potential oral drug delivery system against murine tuberculosis. *Tuberculosis* 2003, 83:373–378. doi:10.1016/j.tube.2003.07.001.

125. Pandey R, Sharma A, Zahoor A, Sharma S, Khuller GK, Prasad B. Poly (DL-lactide-co-glycolide) nanoparticle-based inhalable sustained drug delivery system for experimental tuberculosis. *J Antimicrob Chemother* 2003, 52:981–986. doi:10.1093/jac/dkg477.

126. Sung JC, Padilla DJ, Garcia-Contreras L, VerBerkmoes JL, Durbin D, Peloquin CA, Elbert KJ, Hickey AJ, Edwards DA. Formulation and pharmacokinetics of self-assembled rifampicin nanoparticle systems for pulmonary delivery. *Pharm Res* 2009, 26:1847–1855. doi:10.1007/s11095-009-9894-2.

127. Pandey R, Ahmad Z. Nanomedicine and experimental tuberculosis: facts, flaws, and future. *Nanomedicine* 2011, 7:259–272. doi:10.1016/j.nano.2011.01.009.

128. Lawlor C, Kelly C, O'Leary S, O'Sullivan MP, Gallagher PJ, Keane J, Cryan SA. Cellular targeting and trafficking of drug delivery systems for the prevention and treatment of MTb. *Tuberculosis* 2011, 91:93–97. doi:10.1016/j.tube.2010.12.001.

129. de Faria TJ, Roman M, de Souza NM, De Vecchi R, de Assis JV, dos Santos ALG, Bechtold IH, Winter N, Soares MJ, Silva LP, et al. An isoniazid analogue promotes mycobacterium tuberculosis-nanoparticle interactions and enhances bacterial killing by macrophages. *Antimicrob Agents Chemother* 2012, 56:2259–2267. doi:10.1128/aac.05993-11.

130. Hadinoto K, Sundaresan A, Cheow WS. Lipid-polymer hybrid nanoparticles as a new generation therapeutic delivery platform: a review. *Eur J Pharm Biopharm* 2013, 85:427–443. doi:10.1016/j.ejpb.2013.07.002.

131. Chono S, Tanino T, Seki T, Morimoto K. Influence of particle size on drug delivery to rat alveolar macrophages following pulmonary administration of ciprofloxacin incorporated into liposomes. *J Drug Target* 2006, 14:557–566. doi:10.1080/10611860600834375.

132. Cheow WS, Chang MW, Hadinoto K. The roles of lipid in anti-biofilm efficacy of lipid-polymer hybrid nanoparticles encapsulating antibiotics. *Colloids Surf A* 2011, 389:158–165. doi:10.1016/j.colsurfa.2011.08.035.

133. Liu G, Li DS, Pasumarthy MK, Kowalczyk TH, Gedeon CR, Hyatt SL, Payne JM, Miller TJ, Brunovskis P, Fink TL, et al. Nanoparticles of compacted DNA transfect postmitotic cells. *J Biol Chem*

2003, 278:32578–32586. doi:10.1074/jbc.M305776200.

134. Ziady AG, Gedeon CR, Miller T, Quan W, Payne JM, Hyatt SL, Fink TL, Muhammad O, Oette S, Kowalczyk T, et al. Transfection of airway epithelium by stable PEGylated poly-L-lysine DNA nanoparticles in vivo. *Mol Ther* 2003, 8:936–947. doi:10.1016/j.ymthe.2003.07.007.

135. Pack DW, Hoffman AS, Pun S, Stayton PS. Design and development of polymers for gene delivery. *Nat Rev Drug Discov* 2005, 4:581–593. doi:10.1038/nrd1775.

136. Radovic-Moreno AF, Lu TK, Puscasu VA, Yoon CJ, Langer R, Farokhzad OC. Surface charge-switching polymeric nanoparticles for bacterial cell wall-targeted delivery of antibiotics. *ACS Nano* 2012, 6:4279–4287. doi:10.1021/nn3008383.

137. El-Sherbiny IM, McGill S, Smyth HDC. Swellable microparticles as carriers for sustained pulmonary drug delivery. *J Pharm Sci* 2010, 99:2343–2356. doi:10.1002/jps.22003.

138. El-Sherbiny IM, Smyth HDC. Novel cryomilled physically cross-linked biodegradable hydrogel microparticles as carriers for inhalation therapy. *J Microencapsul* 2010, 27:657–668. doi:10.3109/02652041003739840.

139. Wanakule P, Liu GW, Fleury AT, Roy K. Nano-inside-micro: disease-responsive microgels with encapsulated nanoparticles for intracellular drug delivery to the deep lung. *J Control Release* 2012, 162:429–437. doi:10.1016/j.jconrel.2012.07.026.

140. Xiong M-H, Bao Y, Yang X-Z, Wang Y-C, Sun B, Wang J. Lipase-sensitive polymeric triple-layered nanogel for "on-demand" drug delivery. *J Am Chem Soc* 2012, 134:4355–4362. doi:10.1021/ja211279u.

141. Sharma A, Sharma S, Khuller GK. Lectin-functionalized poly (lactide-co-glycolide) nanoparticles as oral/aerosolized antitubercular drug carriers for treatment of tuberculosis. *J Antimicrob Chemother* 2004, 54:761–766. doi:10.1093/jac/dkh411.

142. Yoo JW, Chambers E, Mitragotri S. Factors that control the circulation time of nanoparticles in blood: challenges, solutions and future prospects. *Curr Pharm Des* 2010, 16:2298–2307. doi:10.2174/138161210791920496.

143. Anselmo AC, Gupta V, Zern BJ, Pan D, Zakrewsky M, Muzykantov V, Mitragotri S. Delivering nanoparticles to lungs while avoiding liver and spleen through adsorption on red blood cells. *ACS Nano* 2013, 7:11129–11137. doi:10.1021/nn404853z.

144. Chambers E, Mitragotri S. Prolonged circulation of large polymeric nanoparticles by non-covalent adsorption on erythrocytes. *J Control Release* 2004, 100:111–119. doi:10.1016/j.jconrel.2004.08.005.

145. Dames P, Gleich B, Flemmer A, Hajek K, Seidl N, Wiekhorst F, Eberbeck D, Bittmann I, Bergemann C, Weyh T, et al. Targeted delivery of magnetic aerosol droplets to the lung. *Nat Nanotechnol* 2007, 2:495–499. doi:10.1038/nnano.2007.217.

146. Cheng CJ, Tietjen GT, Saucier-Sawyer JK, Saltzman WM. A holistic approach to targeting disease with polymeric nanoparticles. *Nat Rev Drug Discov* 2015, 14:239–247. doi:10.1038/nrd4503.

147. Rajendran L, Knölker HJ, Simons K. Subcellular targeting strategies for drug design and delivery. *Nat Rev Drug Discov* 2010, 9:29–42. doi:10.1038/nrd2897.

148. Ding BS, Dziubla T, Shuvaev VV, Muro S, Muzykantov VR. Advanced drug delivery systems that target the vascular endothelium. *Mol Interv* 2006, 6:98–112. doi:10.1124/mi.6.2.7.

149. Chrastina A, Massey KA, Schnitzer JE. Overcoming in vivo barriers to targeted nanodelivery. *WIREs Nanomed Nanobiotechnol* 2011, 3:421–437. doi:10.1002/wnan.143.

150. Massey KA, Schnitzer JE. Targeting and imaging signature caveolar molecules in lungs. *Proc Am Thorac Soc* 2009, 6:419–430. doi:10.1513/pats.200903-011aw.

151. Oh P, Borgström P, Witkiewicz H, Li Y, Borgström BJ, Chrastina A, Iwata K, Zinn KR, Baldwin R, Testa JE, et al. Live dynamic imaging of caveolae pumping targeted antibody rapidly and specifically across endothelium in the lung. *Nat Biotechnol* 2007, 25:327–337. doi:10.1038/nbt1292.

152. Pison U, Welte T, Giersig M, Groneberg DA. Nanomedicine for respiratory diseases. *Eur J Pharmacol* 2006, 533:341–350. doi:10.1016/j.ejphar.2005.12.068.

153. Kudo K, Sano H, Takahashi H, Kuronuma K, Yokota SI, Fujii N, Shimada KI, Yano I, Kumazawa Y, Voelker DR, et al. Pulmonary collectins enhance phagocytosis of mycobacterium avium through increased activity of mannose receptor. *J Immunol* 2004, 172:7592–7602. doi:10.4049/jimmunol.172.12.7592.

154. Chono S, Tanino T, Seki T, Morimoto K. Efficient drug targeting to rat alveolar macrophages by pulmonary administration of ciprofloxacin incorporated into mannosylated liposomes for treatment of respiratory intracellular parasitic infections. *J Control Release* 2008, 127:50–58. doi:10.1016/j.jconrel.2007.12.011.

155. Champion JA, Mitragotri S. Shape induced inhibition of phagocytosis of polymer particles. *Pharm Res* 2009, 26:244–249. doi:10.1007/s11095-008-9626-z.

156. Anselmo AC, Kumar S, Gupta V, Pearce AM, Ragusa A, Muzykantov V, Mitragotri S. Exploiting shape, cellular-hitchhiking and antibodies to

target nanoparticles to lung endothelium: synergy between physical, chemical and biological approaches. *Biomaterials* 2015, 68:1–8. doi:10.1016/j.biomaterials.2015.07.043.

157. Muro S, Garnacho C, Champion JA, Leferovich J, Gajewski C, Schuchman EH, Mitragotri S, Muzykantov VR. Control of endothelial targeting and intracellular delivery of therapeutic enzymes by modulating the size and shape of ICAM-1-targeted carriers. *Mol Ther* 2008, 16:1450–1458. doi:10.1038/mt.2008.127.
158. Nemmar A, Hoylaerts MF, Hoet PHM, Vermylen J, Nemery B. Size effect of intratracheally instilled particles on pulmonary inflammation and vascular thrombosis. *Toxicol Appl Pharm* 2003, 186:38–45. doi:10.1016/S0041-008X(02)00024-8.
159. Hadinoto K, Cheow WS. Nano-antibiotics in chronic lung infection therapy against Pseudomonas aeruginosa. *Colloids Surf B* 2014, 116:772–785. doi:10.1016/j.colsurfb.2014.02.032.
160. Deacon J, Abdelghany SM, Quinn DJ, Schmid D, Megaw J, Donnelly RF, Jones DS, Kissenpfennig A, Elborn JS, Gilmore BF, et al. Antimicrobial efficacy of tobramycin polymeric nanoparticles for pseudomonas aeruginosa infections in cystic fibrosis: formulation, characterisation and functionalisation with dornase alfa (DNase). *J Control Release* 2015, 198:55–61. doi:10.1016/j.jconrel.2014.11.022.
161. Broughton-Head VJ, Smith JR, Shur J, Shute JK. Actin limits enhancement of nanoparticle diffusion through cystic fibrosis sputum by mucolytics. *Pulm Pharmacol Ther* 2007, 20:708–717. doi:10.1016/j.pupt.2006.08.008.
162. Dailey LA, Jekel N, Fink L, Gessler T, Schmehl T, Wittmar M, Kissel T, Seeger W. Investigation of the proinflammatory potential of biodegradable nanoparticle drug delivery systems in the lung. *Toxicol Appl Pharm* 2006, 215:100–108. doi:10.1016/j.taap.2006.01.016.
163. Tahara K, Sakai T, Yamamoto H, Takeuchi H, Hirashima N, Kawashima Y. Improved cellular uptake of chitosan-modified PLGA nanospheres by A549 cells. *Int J Pharm* 2009, 382:198–204. doi:10.1016/j.ijpharm.2009.07.023.
164. Houchin ML, Heppert K, Topp EM. Deamidation, acylation and proteolysis of a model peptide in PLGA films. *J Control Release* 2006, 112:111–119. doi:10.1016/j.jconrel.2006.01.018.
165. Dailey LA, Wittmar M, Kissel T. The role of branched polyesters and their modifications in the development of modern drug delivery vehicles. *J Control Release* 2005, 101:137–149. doi:10.1016/j.jconrel.2004.09.003.
166. Wang XY, Xie XL, Cai CF, Rytting E, Steele T, Kissel T. Biodegradable branched polyesters poly(vinyl sulfonate-covinyl alcohol)-graft poly(D,L-lactic-coglycolic acid) as a negatively charged polyelectrolyte platform for drug delivery: synthesis and characterization. *Macromolecules* 2008, 41:2791–2799. doi:10.1021/ma702705s.
167. Fiore VF, Lofton MC, Roser-Page S, Yang SC, Roman J, Murthy N, Barker TH. Polyketal microparticles for therapeutic delivery to the lung. *Biomaterials* 2010, 31:810–817. doi:10.1016/j.biomaterials.2009.09.100.
168. Fiegel J, Fu J, Hanes J. Poly(ether-anhydride) dry powder aerosols for sustained drug delivery in the lungs. *J Control Release* 2004, 96:411–423. doi:10.1016/j.jconrel.2004.02.018.
169. Fu J, Fiegel J, Krauland E, Hanes J. New polymeric carriers for controlled drug delivery following inhalation or injection. *Biomaterials* 2002, 23:4425–4433. doi:10.1016/s0142-9612(02)00182-5.
170. Salvati A, Pitek AS, Monopoli MP, Prapainop K, Bombelli FB, Hristov DR, Kelly PM, Aberg C, Mahon E, Dawson KA. Transferrin-functionalized nanoparticles lose their targeting capabilities when a biomolecule corona adsorbs on the surface. *Nat Nanotechnol* 2013, 8:137–143. doi:10.1038/nnano.2012.237.
171. Behzadi S, Serpooshan V, Sakhtianchi R, Müller B, Landfester K, Crespy D, Mahmoudi M. Protein corona change the drug release profile of nanocarriers: the "overlooked" factor at the nanobio interface. *Colloids Surf B* 2014, 123:143–149. doi:10.1016/j.colsurfb.2014.09.009.
172. Ritz S, Schöttler S, Kotman N, Baier G, Musyanovych A, Kuharev J, Landfester K, Schild H, Jahn O, Tenzer S, et al. Protein corona of nanoparticles: distinct proteins regulate the cellular uptake. *Biomacromolecules* 2015, 16:1311–1321. doi:10.1021/acs.biomac.5b00108.
173. Tenzer S, Docter D, Kuharev J, Musyanovych A, Fetz V, Hecht R, Schlenk F, Fischer D, Kiouptsi K, Reinhardt C, et al. Rapid formation of plasma protein corona critically affects nanoparticle pathophysiology. *Nat Nanotechnol* 2013, 8:772–781. doi:10.1038/nnano.2013.181.
174. Winzen S, Schoettler S, Baier G, Rosenauer C, Mailaender V, Landfester K, Mohr K. Complementary analysis of the hard and soft protein corona: sample preparation critically effects corona composition. *Nanoscale* 2015, 7:2992–3001. doi:10.1039/c4nr05982d.
175. Kang B, Okwieka P, Schöttler S, Winzen S, Langhanki J, Mohr K, Opatz T, Mailänder V, Landfester K, Wurm FR. Carbohydrate-based nanocarriers exhibiting specific cell targeting with minimum influence from the protein corona. *Angew Chem Int Ed* 2015, 54:7436–7440. doi:10.1002/anie.201502398.

176. Wu Y, Ng DYW, Kuan SL, Weil T. Protein-polymer therapeutics: a macromolecular perspective. *Biomater Sci* 2015, 3:214–230. doi:10.1039/c4bm00270a.

177. Gauthier MA, Klok H-A. Polymer-protein conjugates: an enzymatic activity perspective. *Polym Chem* 2010, 1:1352–1373. doi:10.1039/c0py90001j.

178. Cobo I, Li M, Sumerlin BS, Perrier S. Smart hybrid materials by conjugation of responsive polymers to biomacromolecules. *Nat Mater* 2015, 14:143–149. doi:10.1038/nmat4106.

